

ACon²: Adaptive Conformal Consensus for Provable Blockchain Oracles

Sangdon Park[†]

Osbert Bastani^{*}

Taesoo Kim[†]

[†]*Georgia Institute of Technology*

^{*}*University of Pennsylvania*

Abstract

Blockchains with smart contracts are distributed ledger systems which achieve block state consistency among distributed nodes by only allowing deterministic operations of smart contracts. However, the power of smart contracts is enabled by interacting with stochastic off-chain data, which in turn opens the possibility to undermine the block state consistency. To address this issue, an oracle smart contract is used to provide a single consistent source of external data; but, simultaneously this introduces a single point of failure, which is called the oracle problem. To address the oracle problem, we propose an adaptive conformal consensus (ACon²) algorithm, which derives consensus from multiple oracle contracts via the recent advance in online uncertainty quantification learning. In particular, the proposed algorithm returns a consensus set, which quantifies the uncertainty of data and achieves a desired correctness guarantee in the presence of Byzantine adversaries and distribution shift. We demonstrate the efficacy of the proposed algorithm on two price datasets and an Ethereum case study. In particular, the Solidity implementation of the proposed algorithm shows the practicality of the proposed algorithm, implying that online machine learning algorithms are applicable to address issues in blockchains.

1 Introduction

Blockchains are distributed ledger systems where a set of transactions forms a block, and blocks are securely connected to form a chain via cryptography to avoid record manipulation. The concept of the ledger can be generalized to executable programs, called *smart contracts*, coined by Nick Szabo [40]. As smart contracts can be any program, they provide great amounts of applications of blockchains. In particular, a smart contract is used for providing collateralized lending services within blockchain, *e.g.*, lending USDT via Ethereum. To this end, the contract needs to interact with off-chain data, *e.g.*, an Ethereum price in US Dollars (USD). However, accessing and recording arbitrarily external data in

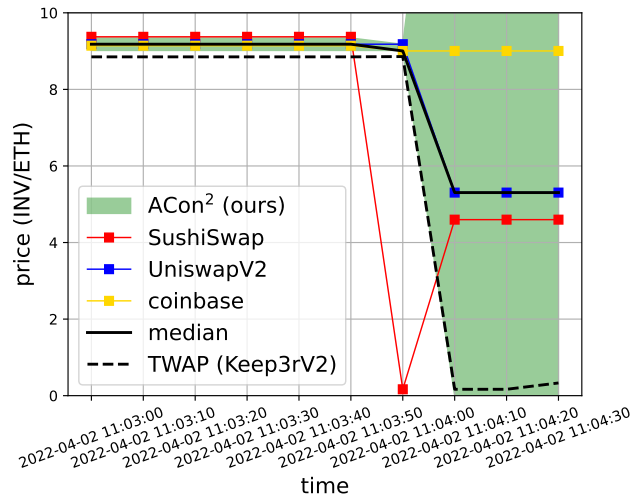


Figure 1: We propose to address prediction consensus via ACon². For an application, we consider the recent price manipulation of an INV token price on SushiSwap. ACon² provides uncertainty on price prediction (in prediction intervals) along with a correctness guarantee under Byzantine adversaries (*e.g.*, price manipulators), resulting in providing large uncertainty after the price manipulation at 2022-04-02 11:03:50 for peculiarity. See Section 6.2 for details.

a blockchain is prohibited due to the deterministic property of distributed blockchains. To maintain consistent block states across distributed nodes, operations in blockchains need to be deterministic. But, reading and writing stochastic data into blockchains break the consistency among blockchains at each distributed node. To avoid this inconsistency issue, a special smart contract, called an *oracle smart contract*, is introduced as a single source of a data feed; however, this in turn provides a single point of failure, called the *oracle problem* [14]. In particular, malicious adversaries can feed invalid data into the oracle contracts to achieve their goals (*e.g.*, price manipulation [15, 20, 27, 28, 36–38, 42], to lend Ethereum with a cheaper price in USDT).

To address the oracle problem, we may use traditional con-

sensus solutions over diverse oracle contracts (*e.g.*, consensus over Byzantine generals [22], consensus over abstract sensors [26], or robust statistics like median or truncated mean). For example, the median prices from diverse price oracle contracts can be used for a consensus price. However, the main challenges to address the oracle problem include the following: handling ❶ the *inevitable uncertainty* in external data for consensus (*e.g.*, ETH/USD price is varying across markets), ❷ the presence of adversaries to undermine consensus, ❸ *distribution shift* along time (*e.g.*, ETH/USD price is varying across time), ❹ a *correctness guarantee* on consensus in dealing with the previous challenges, and ❺ whether the proposed algorithm is implementable in blockchains. To our understanding, these challenges are not jointly considered in a single traditional consensus method.

In this paper, we view the oracle problem as a *prediction consensus learning* problem; we consider each oracle smart contract as a predictor \hat{C}_t at time t , where it predicts the uncertainty over labels y based on the external data observations \mathbf{x}_t . Given multiple predictors from multiple data sources, we learn and predict the consensus over uncertain labels. To address the prediction consensus learning, we exploit the recent advance in online machine learning for uncertainty quantification [3, 18] based on conformal prediction [49].

In particular, we propose an adaptive conformal consensus (ACon²) algorithm that satisfies a correctness guarantee. At time t , this algorithm returns a set-valued predictor \hat{C}_t , where given an observation \mathbf{x}_t from multiple sources, we have a *consensus set* $\hat{C}(\mathbf{x}_t)$ that likely contains the true consensus label even in the presence of adversaries and distribution shift. Here, we model uncertainty via a set over labels, called a *prediction set*, and this set-of-labels notation is equivalent to having multiple votes on labels, *i.e.*, if it is uncertain to choose a one choice, make multiple uncertain choices instead of choosing a one certain but wrong choice; based on this, we can handle uncertainty from data in Challenge ❶. For consensus, we consider that K base prediction sets from K sources are given, and adversaries can arbitrarily manipulate the β sources (thus β base prediction sets) among K , called β -*Byzantine adversaries*. Given K base prediction sets $\hat{C}_{t,k}(\mathbf{x}_t)$ for $k \in \{1, \dots, K\}$, where β of them are possibly manipulated, we construct the consensus set $\hat{C}_t(\mathbf{x}_t)$ that contains labels that are also contained in the $K - \beta$ base prediction sets; by filtering out possibly wrong base prediction sets in this way, the consensus set is not maliciously manipulated by the adversaries, which addresses Challenge ❷. At time t given the observation \mathbf{x}_t along with a label $y_{t,k}$ from the k -th source, the k -th base prediction set $\hat{C}_{t,k}$ is updated via any adaptive conformal prediction (*e.g.*, [3]), which consequently updates the consensus set \hat{C}_t ; as the adaptive conformal prediction learns a correct prediction set under distribution shift, this addresses Challenge ❸. Finally, we provide the worst-case correctness guarantee on the consensus sets from our algorithm ACon²; under any β -Byzantine adversaries and any distribution shift,

the consensus sets from ACon² likely contain the true consensus labels at a desired miscoverage rate. This is proved given the correctness guarantee of the base prediction sets, thus addressing Challenge ❹.

We demonstrate the efficacy of the proposed algorithm ACon² via the evaluation over two datasets and one case study. In particular, we use two datasets, obtained from the Ethereum blockchain: a USD/ETH price dataset, which manifests natural distribution shift, and an INV/ETH price dataset, which embeds price manipulation attacks. For the case study, we implement our algorithm in Solidity to show its practicality on the Ethereum blockchain. In short, we empirically show that the consensus sets by ACon² achieve a desired miscoverage rate even under distribution shift and Byzantine adversaries. Moreover, our Solidity implementation shows that an online machine learning algorithm can be practical to be used in blockchains, which also implying that it can enjoy the underlying security from blockchain-level consensus (*e.g.*, proof-of-work); this addresses Challenge ❺.

2 Background

Here, we provide background on blockchain oracle and online machine learning, in particular adaptive conformal prediction.

2.1 Blockchain Oracles

A blockchain is a distributed ledger system that consists of records, called *blocks*, by securely connecting them in a *chain* via cryptography. The main use of the blockchain is a distributed ledger for cryptocurrencies, like Bitcoin [6] or Ethereum [13]. The concept of the ledger is generalized to record a computer program, called *smart contracts*, practically realized in Ethereum [7]; the smart contracts are automatically executed on the blockchain to provide additional functionalities beyond ledgers, like decentralized finance (DeFi) or a non-fungible token (NFT).

Blockchain oracles. One special type of smart contracts is an *oracle smart contract*. The blockchain is a distributed system, where each node of the system maintains the exactly identical information in a blockchain. To this end, all smart contracts are *deterministic*. However, the blockchain needs to read information from the real world. In particular, Ethereum can be exchanged based on agreed US Dollars (USD) [14], but the value of Ethereum in USD depends on the off-chain *stochastic* data. Thus, by simply reading the stochastic data and feed into on-chain by executing a related smart contract at each node could potentially break the consistency among blockchains at each node.

To address this issue, oracle smart contracts are used to provide a single point of feeding off-chain data; as it is a single point of contact, all smart contracts that interact with it can maintain the consistent blockchain state. However, the

oracle contract can be a single point of failure as well, which is known as the *oracle problem* [14]. To dive into the oracle problem, we first explain one dominant application of smart contracts in DeFi that is heavily related to the oracle problem.

Automated market maker. An automated market maker (AMM) is a smart contract that forms a market to swap tokens. For example, Uniswap [45] is a smart contract protocol that forms AMMs for various pairs of tokens, where the price of tokens is decided by a constant product formula. We take this as our concrete example in describing AMMs. In the constant product formula, the price of a pool of two tokens A and B is decided from the equation $xy = k$ given a constant k , where x and y are the amounts of the token A and token B , respectively. Letting $k = 1$, the current price of the token A by the token B is $\frac{y}{x}$; if a trader sell the token A by the amount of x' , the amount of the token B that the trader will receive is $y' = y - \frac{xy}{x+x'}$ to maintain the ratio of the amounts of two tokens to be $k = 1$. After this trade, the price of the token A by the token B is changed to be $\frac{y-y'}{x+x'}$.

In DeFi, the price formed by an AMM is mainly used for an on-chain decentralized collateralized loaning service. Specifically, a user deposit assets (*e.g.*, ETH) to the lending service to borrow another asset (*e.g.*, USD in USDT) proportional to the value of the deposited assets. Taking an example from [38], suppose the collateralization ratio is 150%. If the spot price (*i.e.*, the current price which can be sold immediately) of ETH is 400 USD, the user can borrow 100,000 USD by the deposit of 375 ETH, *i.e.*,

$$375 \text{ (ETH)} \times 400 \left(\frac{\text{USD}}{\text{ETH}} \right) \times \frac{100}{150} = 100,000 \text{ (USD)} \quad (1)$$

To get the spot price of ETH, the lending service accesses to a price oracle, possibly from an AMM.

The oracle problem and oracle manipulation. The *oracle problem* is a contradictory situation where a blockchain needs a single oracle smart contract that reads data from off-chain to maintain consistency among distributed blockchains, while the oracle contract can be a point of failure by *manipulation*. For example, the price formed by the AMM reflects the value of two tokens in the real world, thus the smart contract that provides a price is also the oracle contract. But, considering the way to decide a price in AMMs, it is susceptible to price manipulation. In particular, an adversary can sell a huge amount of token A to an AMM, then its price at this AMM is skewed compared to the price of other AMMs, thus maliciously affecting other DeFi services that rely on the price from the manipulated AMM.

The price manipulation has been actually executed [15, 20, 27, 28, 36–38, 42], even recently [36] on April 2 in 2022 when we write this paper at October in 2022. Here, we provide a simplified price manipulation attack from [38]; see [37] for detailed analysis. Suppose the spot price of 1 ETH is

400 USD at Uniswap. An adversary buys 5,000 ETH for 2,000,000 USD from Uniswap. The spot price of 1 ETH is now 1,733.33 USD at Uniswap. The lending service fetches the spot price of ETH from Uniswap, which is 1 ETH = 1,733.33 USD. The adversary can borrow 433,333.33 USD by depositing 375 ETH, which is about four times higher before the price manipulation in (1). Then, the adversary sell 5,000 ETH for 2,000,000 USD to return back to the original price. This attack can be implemented to be atomic, so arbitrage is not possible. Thus, the attacker enjoys the benefit by 333,333.33 USD.

Countermeasures. Practical countermeasures to defend against price manipulation have been proposed [8, 46]. Assuming a single price source is given, we can consider the average price within a time frame, *i.e.*, $\frac{C_{t_1} - C_{t_0}}{t_1 - t_0}$, where t_0 is the previous timestamp, t_1 is the current timestamp, C_{t_0} is the previous cumulative price, and C_{t_1} is the current cumulative price. This is called Time-Weighted Average Price (TWAP) [46]. Here, the time frame $t_1 - t_0$ is a design parameter; if it is large, the TWAP is hard to manipulate as the manipulated price is exposed to arbitrage opportunities and also the aggressively manipulated price is averaged out. However, the choice of the large time frame sacrifices getting an up-to-date price. If the time frame is set by a relatively small value, the price is heavily affected by the manipulation, which is the main cause of the recent Inverse Finance incident [36]. Alternatively, when multiple price sources are given, we can consider price accumulation among multiple sources; one traditional way is considering robust statistics, *e.g.*, the median among prices; Chainlink [8] uses the median approach in sophisticated ways.

The known practical solutions are considered to have limitations on guaranteeing security. In particular, TWAP assumes to set the right time frame, and the median robust statistics does not provide the likelihood of the correctness on the median value. Instead, we rely on machine learning theories, in particular online machine learning and conformal prediction, to handle the oracle problem with provable correctness guarantees by learning security sensitive parameters.

2.2 Adaptive Conformal Prediction

Uncertainty quantification on prediction is essential to build trustworthy predictors. Conformal prediction provides a rigorous way to provide the correctness guarantee on quantified uncertainty via prediction sets (*i.e.*, a set of predicted labels). The conformal prediction originally assumes a distribution on data is not changing (more precisely exchangeability), but the recent work [3, 18] extends this to handle distribution shift, making it more applicable in practical settings.

We describe a setup for adaptive conformal prediction, which is an online machine learning variant of the conformal prediction. Let \mathcal{X} be example space, \mathcal{Y} be label space,

and \mathcal{P}' be the set of all distribution over $\mathcal{X} \times \mathcal{Y}$. In conformal prediction, we assume that a conformity score function $s_t : \mathcal{X} \times \mathcal{Y} \rightarrow \mathbb{R}_{\geq 0}$ at time $t \in \{1, \dots, T\}$ for a time horizon T is given, which measures whether datum $(x, y) \in \mathcal{X} \times \mathcal{Y}$ conforms to a score function s_t . Then, a prediction set $\hat{C}_t \in 2^{\mathcal{Y}}$ at time t is constructed based on the score function as follows:

$$\hat{C}_t(x) := \{y \in \mathcal{Y} \mid s_t(x, y) \geq \tau_t\}, \quad (2)$$

where $\tau_t \in \mathbb{R}_{\geq 0}$ is a parameter of the prediction set, and we denote a set of all prediction sets by \mathcal{F}' .

The main goal of adaptive conformal prediction is choosing τ_t at time t such that a prediction set \hat{C}_t likely contains the true label y_t . To measure the goodness of prediction sets, we use the miscoverage of the prediction set, defined as follows:

$$Miscover(\hat{C}_t, x, y) := \mathbb{1}(y \notin \hat{C}_t(x)).$$

In adaptive conformal prediction, we desire to find a learner L that uses all previous data and prediction sets, such that the learner returns a distribution over prediction sets where sampled prediction sets achieve a desired miscoverage rate α on the worst-case data during time until T ; the mistakes of the learner is measured by a miscoverage value \mathcal{V}' as follows:

$$\begin{aligned} \mathcal{V}'(\mathcal{F}', T, \alpha, L) := \max_{p_1 \in \mathcal{P}'} \mathbb{E}_{(X_1, Y_1) \sim p_1} \dots \max_{p_T \in \mathcal{P}'} \mathbb{E}_{(X_T, Y_T) \sim p_T} \\ \left| \frac{1}{T} \sum_{t=1}^T Miscover(\hat{C}_t, X_t, Y_t) - \alpha \right|, \quad (3) \end{aligned}$$

where the max over distributions contributes to generate the worst-case data that lead the prediction sets to miscover the data. We say that a learner L is (α, ε) -correct for \mathcal{F}' and T if

$$\mathcal{V}'(\mathcal{F}', T, \alpha, L) \leq \varepsilon.$$

The correctness of this base learner is used as a building block to address the blockchain oracle problem.

3 Prediction Consensus

We view the blockchain oracle problem as prediction consensus under Byzantine adversaries and distribution shift, where we find a consensus learner based on multiple data sources. Figure 2 summarizes our problem and its application to price consensus. In the following, we consider our setups on the nature, an adversary, and a consensus learner.

3.1 Setup

3.1.1 Nature

We have multiple sources, from which data is fed into a blockchain. In particular, let K be the number of sources, \mathcal{X}_k be the example space of the k -th source, and \mathcal{Y} be

the label space, shared by all sources. Here, we consider $(\mathbf{x}_{t,k}, \mathbf{y}_{t,k}) \in \mathcal{X}_k \times \mathcal{Y}$ as a datum from the k -th source at time $t \in \{1, \dots, T\}$, where H is a time horizon. Additionally, let $\mathcal{X} := \mathcal{X}_1 \times \dots \times \mathcal{X}_K$ be the example space from all sources and $\mathcal{Y} := \mathcal{Y}^K$ be the label space from all sources, where we consider $(\mathbf{x}_t, \mathbf{y}_t) := (\mathbf{x}_{t,1}, \dots, \mathbf{x}_{t,K}, \mathbf{y}_{t,1}, \dots, \mathbf{y}_{t,K}) \in \mathcal{X} \times \mathcal{Y}$ as a datum from all sources at time t . Finally, let y_t be a consensus label at time t . Importantly, this consensus label is generally not observable. For example, the consensus price of AMMs forms when the reserves of tokens are infinite, which we cannot observe. But, the price that we observe forms based on the finite reserves.

To address the prediction consensus problem, we aggregate labels from the K -sources to estimate the consensus label. However, as labels embed uncertainty, we need an uncertainty-aware consensus scheme. To quantify the uncertainty, we consider a set of distributions over $\mathcal{X} \times \mathcal{Y} \times \mathcal{Y}$, denoted by \mathcal{P} . In particular, given a distribution $p_t \in \mathcal{P}$ at time t , we have a datum $(\mathbf{x}_t, \mathbf{y}_t, y_t)$ sampled from p_t , where we consider random variables as upper-case letters, *i.e.*, $(\mathbf{X}_t, \mathbf{Y}_t, Y_t) \sim p_t$.

As the consensus label y_t is not generally observable, we connect it from the K labels based on the structural information from the following assumption on the consensus label and source labels; we assume that the consensus label distribution is identical to the label distribution of each source.

Assumption 1. Assume $p_t(\mathbf{y}_{t,k} \mid \mathbf{x}_t) = p_t(y_t \mid \mathbf{x}_t)$ for any $t \in \{1, \dots, T\}$ and $k \in \{1, \dots, K\}$.

A good example that justifies this assumption is the existence of arbitrage in price markets; as arbitrage balances prices across markets, we can assume that a consensus price y_t tends to match to a local price $\mathbf{y}_{t,k}$. Note that this assumption can be relaxed; see Section 8 on the discussion for a weaker assumption. Additionally, we assume the conditional independence of source labels $\mathbf{y}_{t,k}$ and a consensus label y_t given observations \mathbf{x}_t .

Assumption 2. Assume $\prod_{k=1}^K p_t(\mathbf{y}_{t,k} \mid \mathbf{x}_t) = p_t(\mathbf{y}_t \mid \mathbf{x}_t, y_t)$ for any $t \in \{1, \dots, T\}$ and $k \in \{1, \dots, K\}$.

3.1.2 Adversary

We consider Byzantine adversaries. In particular, let $e_t : \mathcal{X} \rightarrow \mathcal{X}$ be a Byzantine adversary that arbitrarily manipulates examples from arbitrarily chosen sources. Here, we assume to know that β sources are manipulated, but we don't know which β sources are chosen by the adversary.

Definition 1 (threat model). *An adversary $e_t : \mathcal{X} \rightarrow \mathcal{X}$ at time t is a β -Byzantine adversary if the adversary arbitrarily manipulates β sources among all sources.*

We denote a set of all β -Byzantine adversaries by \mathcal{E}_β . In blockchains, price manipulation adversaries can be considered as Byzantine adversaries.

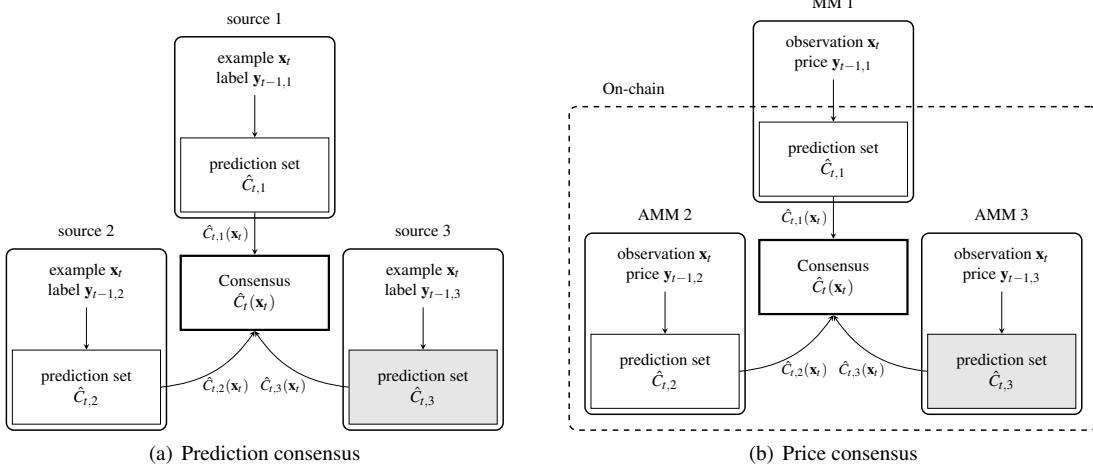


Figure 2: Prediction consensus and its application to price consensus. In prediction consensus, we aim to construct a consensus set \hat{C}_t that likely contains a consensus label even under the Byzantine adversaries (as shown in gray) and distribution shift, which undermine the consensus. The consensus set is constructed based on votings from base prediction sets $\hat{C}_{t,1}$, $\hat{C}_{t,2}$, and $\hat{C}_{t,3}$ from multiple data sources. Each base prediction sets are updated via online machine learning, thus the consensus set is also indirectly updated based on data from each source.

3.1.3 Consensus Learner

This paper considers a set-valued predictor to model prediction consensus. In particular, let $\hat{C}_t : \mathcal{X} \rightarrow 2^{\mathcal{Y}}$ be a consensus set, where it takes examples from K -sources at time t to predict consensus labels as a set. Here, we denote the collection of prediction consensus sets by \mathcal{F} . Importantly, we consider the set-valued predictor instead of a point-estimator to explicitly model the uncertainty of the prediction.

At time t , given all previous data $(\mathbf{x}_i, \mathbf{y}_i)$ and prediction consensus sets \hat{C}_i for $1 \leq i \leq t-1$, i.e., $\mathbf{z}_{1:t-1} := (\mathbf{x}_1, \dots, \mathbf{x}_{t-1}, \mathbf{y}_1, \dots, \mathbf{y}_{t-1}, \hat{C}_1, \dots, \hat{C}_{t-1})$, we design a learner $L : (\mathcal{X} \times \mathcal{Y} \times \mathcal{F})^* \rightarrow Q$ that returns a distribution over prediction consensus sets \mathcal{F} for the future time step¹. As we desire to design a learner L that satisfies a correctness guarantee even in the presence of Byzantine adversaries and distribution shift, we consider the following correctness definition adopted from online machine learning [35]. In particular, letting T be a time horizon and α be a desired miscoverage rate, we denote the miscoverage value of the prediction consensus learner L under β -Byzantine adversaries and distribution shift by $\mathcal{V}(\mathcal{F}, T, \alpha, \beta, L)$, where

$$\begin{aligned} \mathcal{V}(\mathcal{F}, T, \alpha, \beta, L) := & \max_{\substack{p_1 \in \mathcal{P} \\ e_1 \in \mathcal{E}_\beta}} \mathbb{E} \dots \max_{\substack{p_T \in \mathcal{P} \\ e_T \in \mathcal{E}_\beta}} \mathbb{E} \\ & \frac{1}{T} \sum_{t=1}^T \text{Miscover}(\hat{C}_t, e_t(\mathbf{X}_t), Y_t) - \alpha. \end{aligned} \quad (4)$$

Here, the t -th expectation is taken over $\mathbf{X}_t \sim p_t(\mathbf{x})$, $\mathbf{Y}_t \sim p_t(\mathbf{y} \mid e_t(\mathbf{X}_t))$, $Y_t \sim p_t(y \mid \mathbf{X}_t)$, and $\hat{C}_t \sim L(\mathbf{z}_{1:t-1})$. Intuitively, the max over distributions \mathcal{P} models the worst-case distribution

¹ $S^* := \bigcup_{i=0}^{\infty} S^i$.

shift, and the max over \mathcal{E}_β models the worst-case Byzantine adversaries. Moreover, we consider that the consensus label is not affected by the adversaries, as represented in $Y_t \sim p_t(y \mid \mathbf{X}_t)$, while the source label can be affected by the adversaries e_t , as in $\mathbf{Y}_t \sim p_t(\mathbf{y} \mid e_t(\mathbf{X}_t))$. Note that a learner L cannot observe a consensus label Y_t , but Y_t is only used for evaluating the learner via the value \mathcal{V} .

Considering the value of a learner as a correctness criterion, we aim to design a learner that is correct under Byzantine adversaries and distribution shift.

Definition 2 (correctness). *A learner $L : (\mathcal{X} \times \mathcal{Y} \times \mathcal{F})^* \rightarrow Q$ is $(\alpha, \beta, \varepsilon)$ -correct for \mathcal{F} and T if we have*

$$\mathcal{V}(\mathcal{F}, T, \alpha, \beta, L) \leq \varepsilon.$$

This correctness definition does not consider the size of prediction consensus set; if a learner can return prediction sets that output the entire label set, this learner is always correct, but its uncertainty measured by the set size is not informative. So, we also consider to minimize the prediction set size $S(\hat{C}_t, e_t(\mathbf{x}_t))$ at time t based on some application specific size metric $S : \mathcal{Y} \rightarrow \mathbb{R}_{\geq 0}$. Note that the miscoverage value \mathcal{V}' in (3) accounts for the size by considering the absolute value on the difference of the miscoverage rate and a desired miscoverage; this may require a scalar parameterization of a prediction set as in (2), but we consider a general setup to cover various adaptive conformal predictors.

3.2 Problem

In this paper, we view the blockchain oracle problem as a prediction consensus problem; in particular, for any given \mathcal{F} , T , ε , α , and β , we find an $(\varepsilon, \alpha, \beta)$ -correct consensus learner,

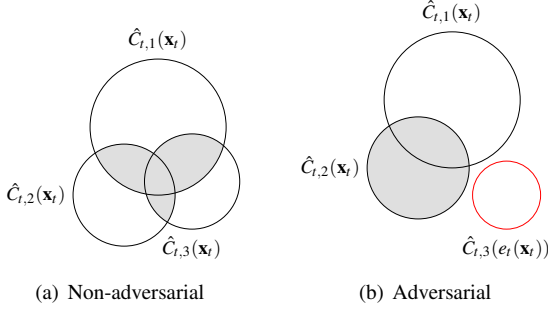


Figure 3: Prediction consensus at time t , where $K = 3$ and $\beta = 1$. The consensus set is a set of labels voted by $K - \beta$ prediction sets as highlighted in gray. Without adversarial manipulation as in Figure 3(a), a consensus label is likely to be contained in the consensus set due to the correctness of base prediction sets; in the presence of adversarial manipulation as in Figure 3(b), the consensus label is still likely to be contained in the consensus set as the majority of prediction sets are still probably correct.

while minimizing the size of prediction sets across time. The main challenges include ①, ②, ③, ④, and ⑤.

4 Adaptive Conformal Consensus

We propose an *adaptive conformal consensus* (ACon²) approach for prediction consensus under Byzantine adversaries and distribution shift. Intuitively, our approach aggregates votes on labels from base prediction sets to form a consensus set, a set of labels if they are voted from at least $K - \beta$ base prediction sets. We provide the correctness guarantee on the consensus set, *i.e.*, the consensus set probably contains the true consensus label even if β of K base prediction sets are arbitrarily manipulated by Byzantine adversaries and even under distribution shift; this guarantee relies on the correctness guarantee of the base prediction sets.

4.1 Consensus Sets

We define a consensus set, a set-valued function to handle uncertainty to address Challenge ①. In particular, given base prediction sets $\hat{C}_{t,k}$ for $k \in \{1, \dots, K\}$ at time t , the consensus set \hat{C}_t contains a label if it is included in at least $K - \beta$ base prediction sets, as follows:

$$\hat{C}_t(\mathbf{x}_t) := \left\{ y \in \mathcal{Y} \mid \sum_{k=1}^K \mathbb{1}(y \in \hat{C}_{t,k}(\mathbf{x}_t)) \geq K - \beta \right\}. \quad (5)$$

Figure 3 illustrates two examples on consensus sets without and with Byzantine adversaries. In particular, Figure 3(a) shows the a consensus set highlighted in a gray area; if each base prediction set contains the consensus label for sure, their intersection should contain the consensus label. However, we cannot guarantee that each base prediction set must contain

the consensus label, but intuitively, if each base prediction set *probably* contains the consensus label, their intersection might be as well. Figure 3(b) illustrates a consensus set, assuming one base prediction set is arbitrarily manipulated. As can be seen, the adversarial manipulation does not introduce new labels compared to the original consensus set in Figure 3(a), meaning that the adversarial manipulation does not maliciously affect the consensus by introducing new labels.

Here, we suppose that the base prediction sets $\hat{C}_{t,k}$ that satisfies a correctness property are given at time t . In Section 4.2, we introduce a way to construct the base prediction sets. Moreover, we can view that the consensus set is based on a special conformity score $\sum_{k=1}^K \mathbb{1}(y \in \hat{C}_{t,k}(\mathbf{x}_t))$, thus also denoting it by conformal consensus sets.

Algorithm 1 Adaptive Conformal Consensus (ACon²)

```

1: for  $t = 1, \dots, T$  do
2:   Observe  $\mathbf{x}_t$ 
3:   Construct a consensus set  $\hat{C}_t(\mathbf{x}_t)$  via (5)
4:   for  $k = 1, \dots, K$  do
5:     Observe  $\mathbf{y}_{t,k}$ 
6:      $\hat{C}_{t+1,k} \leftarrow \text{update}(\hat{C}_{t,k}, \mathbf{x}_t, \mathbf{y}_{t,k})$ 

```

Algorithm. To construct a consensus set, we propose a meta algorithm, which uses prediction sets constructed from each source. In particular, at time t the algorithm observes \mathbf{x}_t , from which K source prediction sets, it constructs a consensus set via (5). Once each source prediction set observes a label $\mathbf{y}_{t,k}$, it is updated via a base prediction set algorithm, from which the consensus set is also updated. The proposed meta algorithm is described in Algorithm 1, which we denote by *Adaptive Conformal Consensus* (ACon²). An update function $\text{update}(\cdot)$ in Line 6 consists of two update functions, *i.e.*, the update on $\hat{C}_{t,k}$ by an adaptive conformal prediction, denoted by $\text{update}_{\text{ACP}}(\cdot)$, and the update on the score function of $\hat{C}_{t,k}$ by a conventional online learning algorithm, denoted by $\text{update}_{\text{score}}(\cdot)$. Here, we consider the following update, but the order of update is not critical: $\text{update}(\hat{C}, \mathbf{x}, \mathbf{y}) = \text{update}_{\text{score}}(\text{update}_{\text{ACP}}(\hat{C}, \mathbf{x}, \mathbf{y}), \mathbf{x}, \mathbf{y})$. Note that enumerating over \mathcal{Y} to construct the consensus set is not trivial depending on the score function if \mathcal{Y} is continuous; see Section 5 for details.

Theory. The consensus set constructed by Algorithm 1 is correct under Byzantine adversaries and distribution shift. This correctness is based on the correctness of each base prediction set and consensus among them. In particular, each base prediction set is updated via an online machine learning algorithm, which guarantees to learn a prediction set from sequential data even if the data is adversarially chosen to fool the algorithm. One benefit of this adaptiveness is that the algorithm learns distribution shift (*i.e.*, global shift), while the downside is that it also learns adversarial shift (*i.e.*, local shift). For

example, when the price of a token pair is manipulated, the algorithm learns the pattern from the manipulated price and considers the price is correct. By only using the online learning algorithm, we cannot distinguish local shift (e.g., price manipulation) and global shift (e.g., consistent price drop). To overcome this limitation of each base prediction set, we consider the consensus among base prediction sets, such that local shift does not affect the consensus.

First, consider the miscoverage value of each base learner L_k for the k -th source. Specifically, at time $t \in \{1, \dots, T\}$, the k -th source can be manipulated by a β -Byzantine adversary e_t , thus an example \mathbf{X}_t and the corresponding label $\mathbf{Y}_{t,k}$ are manipulated. The learner $L_k : (\mathcal{X} \times \mathcal{Y} \times \mathcal{F}_k)^* \rightarrow Q_k$ uses observed normal or manipulated labeled examples $(\mathbf{x}'_1, \mathbf{y}'_{1,k}), \dots, (\mathbf{x}'_{t-1}, \mathbf{y}'_{t-1,k})$ along with the previous prediction sets $\hat{C}_{1,k}, \dots, \hat{C}_{t-1,k}$ to find a distribution over prediction sets such that a prediction set $\hat{C}_{t,k}$ drawn from this distribution achieves a desired miscoverage rate α_k . Similar to the miscoverage value of the consensus learner in (4), we define the miscoverage value of each base learner as follows:

$$\begin{aligned} \mathcal{V}_k(\mathcal{F}_k, T, \alpha_k, \beta, L_k) &:= \max_{p_1 \in \mathcal{P}} \dots \max_{p_T \in \mathcal{P}} \\ &\quad e_1 \in \mathcal{E}_\beta \quad e_T \in \mathcal{E}_\beta \\ &\quad \frac{1}{T} \sum_{t=1}^T \text{Miscover}(\hat{C}_{t,k}, e_t(\mathbf{X}_t), \mathbf{Y}_{t,k}) - \alpha_k, \quad (6) \end{aligned}$$

where the t -th expectation is taken over $\mathbf{X}_t \sim p_t(\mathbf{x})$, $\mathbf{Y}_{t,k} \sim p_t(y | e_t(\mathbf{X}_t))$, and $\hat{C}_{t,k} \sim L_k(\mathbf{z}_{1:t-1})$. Suppose that the miscoverage value of the base learner is bounded by $\varepsilon_{T,k}$:

$$\mathcal{V}_k(\mathcal{F}_k, T, \alpha_k, \beta, L_k) \leq \varepsilon_{T,k}.$$

We prove that the miscoverage value of a consensus set constructed by Algorithm 1 is bounded even under β Byzantine adversaries and distribution shift, suggesting that the consensus set eventually achieves a desired miscoverage rate; see Appendix A.3 for a proof.

Theorem 1. *A consensus learner L satisfies*

$$\mathcal{V}\left(\mathcal{F}, T, \sum_{k=1}^K \alpha_k, \beta, L\right) \leq \sum_{k=1}^K \varepsilon_{T,k}$$

if a base learner L_k for any $k \in \{1, \dots, K\}$ satisfies

$$\mathcal{V}_k(\mathcal{F}_k, T, \alpha_k, \beta, L_k) \leq \varepsilon_{T,k}.$$

Intuitively, the miscoverage value of the proposed consensus learner is bounded by the sum of the miscoverage value bounds of its base learners. This means that if the value of each base learner is bounded by a decreasing function, the consensus learner does as well, implying it eventually converges to a desired miscoverage $\sum_{k=1}^K \alpha_k$, even under β -Byzantine adversaries and distribution shift. This theorem proves that the proposed consensus learner is $(\sum_{k=1}^K \alpha_k, \beta, \sum_{k=1}^K \varepsilon_{T,k})$ -correct for \mathcal{F} and T ; thus, this addresses Challenge ②, ③, and ④.

Theorem 1 assumes that the bound of each base learner's miscoverage value \mathcal{V}_k are known. Here, we connect this value to known miscoverage values \mathcal{V}' in (3) of adaptive conformal prediction. In particular, if the miscoverage value of adaptive conformal prediction is bounded, our miscoverage value of a base learner under Byzantine adversaries is also bounded using the same algorithm; see Appendix A.4 for a proof.

Lemma 1. *We have $\mathcal{V}_k(\mathcal{F}_k, T, \alpha_k, \beta, L_k) \leq \mathcal{V}'(\mathcal{F}_k, T, \alpha_k, L_k)$.*

On the choice of β . Importantly, Theorem 1 holds for any β , suggesting that the correctness does not depend on the parameter of the Byzantine adversaries. However, assuming stronger adversaries (i.e., larger β) produces larger prediction sets due to (5). Thus, we recommend to choose $\beta = \lfloor \frac{K}{2} \rfloor$, assuming the half sources are not manipulated.

Implications. We highlight the implication of Byzantine robustness. In particular, at time t , less than K observations can be made (e.g., by the failure of some base prediction sets). In this case, we can consider the missing observation as the result of the Byzantine adversaries, thus the correctness guarantee in Theorem 1 still holds. Interestingly, in the context of blockchains, if all sources of base prediction sets are from on-chain information (e.g., base prediction sets from AMMs), we can enjoy the lower-level consensus mechanism (e.g., proof-of-work) to have reliable base prediction sets.

4.2 Base Prediction Sets

The proposed adaptive conformal consensus is used with *any* (α, ε) -correct adaptive conformal prediction for constructing base prediction sets. The following includes possible options for blockchain applications, where computational efficiency is one of critical measures.

4.2.1 A Score Function for Regression

The conformal prediction is generally used with any application-dependent score function. Considering that our main application in blockchains is price regression, we propose to use the Kalman filter [21] as a score function. In particular, the Kalman filter is used to estimate states based on the sequence of observations. Here, we use it to estimate price based on the previous price data. In the Kalman filter, we consider a price datum $y_{t,k}$ as an observation from the k -th source at time t , from which we estimate the price state. To this end, we have the identity matrices as an observation model and state-transition model. Moreover, let $w_{t,k}^2$ be the variance of zero-mean state Gaussian noise, and $v_{t,k}^2$ be the variance of zero-mean observation Gaussian noise.

Prediction. At time t before observing the price $y_{t,k}$, the Kalman filter can be used to predict the distribution over

observations given the previous data $\mathbf{y}_{1,k}, \dots, \mathbf{y}_{t-1,k}$ as follows:

$$\mathcal{N}(\mu_{t-1,k}, \sigma_{t-1,k}^2 + w_{t-1,k}^2 + v_{t-1,k}^2),$$

where $\mathcal{N}(\mu, \sigma^2)$ is the Gaussian distribution with the mean of μ and the variance of σ^2 , $\mu_{t-1,k}$ and $\sigma_{t-1,k}^2$ are estimated from $\mathbf{y}_{1,k}, \dots, \mathbf{y}_{t-1,k}$ via the Kalman prediction. This prediction over observations is used for the score function $s_{t,k}$. In particular, let $\mathbf{x}_t := (\mathbf{y}_{1,k}, \dots, \mathbf{y}_{t-1,k})$ be an example from the k -th source at time t , which is a list of price data up to time $t-1$. Then, we define the score function $s_{t,k}$ by the Gaussian distribution over observations, which measures how likely $\mathbf{y}_{t,k}$ will be observed at time t , *i.e.*,

$$s_{t,k}(\mathbf{x}_t, \mathbf{y}_{t,k}) := \mathcal{N}(\mathbf{y}_{t,k}; \mu_{t-1,k}, \sigma_{t-1,k}^2 + w_{t-1,k}^2 + v_{t-1,k}^2),$$

where $\mathcal{N}(y; \mu, \sigma^2)$ denotes the probability of y over $\mathcal{N}(\mu, \sigma^2)$. Note that we assume that the k -th source only uses $\mathbf{x}_{t,k}$, but this can be generalized to use the entire \mathbf{x}_t from all sources.

Update. After observing $\mathbf{y}_{t,k}$, the score function $s_{t,k}$ is updated in two ways: noise update and Kalman update. For the noise update, we conduct gradient descent update on noise variances $w_{t-1,k}$ and $v_{t-1,k}$, which minimizes the negative log-likelihood of the score function on an observation, *i.e.*, $\ell(w_{t-1,k}, v_{t-1,k}) := -\ln s_{t,k}(\mathbf{x}_t, \mathbf{y}_{t,k})$. Letting γ_{noise} be the learning rate of noise parameters, we update noise variances $w_{t,k}$ and $v_{t,k}$ as follows:

$$\begin{aligned} \text{update}_{\text{noise}}(\hat{C}, \mathbf{x}_t, \mathbf{y}_{t,k}) : \quad w_{t,k} &\leftarrow w_{t-1,k} - \gamma_{\text{noise}} \nabla_w \\ v_{t,k} &\leftarrow v_{t-1,k} - \gamma_{\text{noise}} \nabla_v, \end{aligned}$$

where

$$\begin{aligned} \nabla_w &= -2w_{t-1,k} \left(\frac{1}{\xi} - \frac{(\mathbf{y}_{t,k} - \mu_{t-1,k})^2}{\xi^3} \right) \left(\frac{1}{\xi} - \frac{\sigma_{t-1,k}^2 + w_{t-1,k}^2}{2\xi^3} \right), \\ \nabla_v &= 2v_{t-1,k} \left(\frac{1}{\xi} - \frac{(\mathbf{y}_{t,k} - \mu_{t-1,k})^2}{\xi^3} \right) \left(\frac{\sigma_{t-1,k}^2 + w_{t-1,k}^2}{2\xi^3} \right), \end{aligned}$$

and $\xi := \sqrt{\sigma_{t-1,k}^2 + w_{t-1,k}^2 + v_{t-1,k}^2}$. Here, ∇_w or ∇_v is the gradient of $\ell(w_{t-1,k}, v_{t-1,k})$ with respect to $w_{t-1,k}$ or $v_{t-1,k}$.

For the state update, via the Kalman update, the state Gaussian distribution $\mathcal{N}(\mu_{t,k}, \sigma_{t,k}^2)$ is updated as follows:

$$\begin{aligned} \text{update}_{\text{Kalman}}(\hat{C}, \mathbf{x}_t, \mathbf{y}_{t,k}) : \quad \mu_{t,k} &\leftarrow \mu_{t-1,k} - K_t(\mathbf{y}_{t,k} - \mu_{t-1,k}) \\ \sigma_{t,k}^2 &\leftarrow (1 - K_t)(\sigma_{t-1,k}^2 + w_{t-1,k}^2), \end{aligned}$$

where $K_t = (\sigma_{t-1,k}^2 + w_{t-1,k}^2) / (\sigma_{t-1,k}^2 + w_{t-1,k}^2 + v_{t-1,k}^2)$. Based on the two update functions, we can define the update for the score function as follows: $\text{update}_{\text{score}}(\hat{C}, \mathbf{x}, \mathbf{y}) = \text{update}_{\text{Kalman}}(\text{update}_{\text{noise}}(\hat{C}, \mathbf{x}, \mathbf{y}), \mathbf{x}, \mathbf{y})$.

Pros and cons. Sequential data can be learned via non-linear filtering approaches (*e.g.*, extended Kalman or particle filtering) or recurrent neural networks. Compared to

these, the Kalman filter is computationally light, preferred in blockchains. The downside of the Kalman filter is its strong Gaussian assumption. However, this assumption does not affect the correctness of base prediction sets and also consensus sets, while affecting the size of sets.

4.2.2 Adaptive Conformal Prediction

Given a score function $s_{t,k}$ and a labeled example $(\mathbf{x}_t, \mathbf{y}_{t,k})$ at time t , the k -th base prediction set is updated via adaptive conformal prediction. Here, we consider a specific algorithm, called multi-valid conformal prediction (MVP), where we use a special variation of MVP (*i.e.*, MVP with a single group).

Prediction. MVP considers that the prediction set parameter $\tau_{t,k}$ is roughly quantized via binning. Let m be the number of bins, τ_{\max} is the maximum value of $\tau_{t,k}$, $B_i = [\tau_{\max} \frac{i-1}{m}, \tau_{\max} \frac{i}{m})$, and $B_m = [\tau_{\max} \frac{m-1}{m}, \tau_{\max}]$. We consider a prediction set parameterized by $\tau_{t,k}$, which falls in the one of these bins, *i.e.*, $\hat{C}_{t,k}(\mathbf{x}_t) := \{y \in \mathcal{Y} \mid s_{t,k}(\mathbf{x}_t, y) \geq \tau_{t,k}\}$. Moreover, we consider that $\hat{C}_{t,k}$ representation includes internal states $n_{t,k} \in \mathbb{R}^m$ and $v_{t,k} \in \mathbb{R}^m$, initialized zero and updated as the algorithm observes labeled examples $(\mathbf{x}_t, \mathbf{y}_{t,k})$. In prediction, we generate $\hat{C}_{t,k}(\mathbf{x}_t)$ as an input for the consensus set. Here, enumerating over \mathcal{Y} is not trivial if \mathcal{Y} is continuous; see Section 5 for details.

Update. Algorithm 2 in Appendix B updates $n_{t,k}$ and $v_{t,k}$, and compute $\tau_{t,k}$ to update $\hat{C}_{t,k}$ given learning rate η . Here, *rand()* randomly chooses a real number in $[0, 1)$. We use $\text{update}_{\text{MVP}}$ for $\text{update}_{\text{ACP}}$.

Correctness. The MVP learner by Algorithm 2 is (ϵ, α) -correct for a set of quantized thresholds and T . In particular, the correctness bound of the MVP in [3] is proved for a multi-valid guarantee. Here, we explicitly connect that the MVP bound is used to bound the miscoverage value of the MVP learner as follows (see Appendix A.5 for a proof):

Lemma 2. *Letting $S_i = \{t \in \{1, \dots, T\} \mid \tau_{t,k} \in B_i\}$, the MVP learner L_{MVP} satisfies the following:*

$$\mathcal{V}'(\mathcal{F}, T, \alpha, L_{\text{MVP}}) \leq \sum_{i=1}^m \frac{f(|S_i|)}{|S_i|} \sqrt{13.6m \ln m}$$

if a distribution over scores $s_t(X_t, Y_t)$ for any $t \in \{1, \dots, T\}$ is smooth enough² and $\sqrt{\frac{\ln m}{6.8m}} \leq \eta \leq \sqrt{\frac{\ln m}{6.6m}}$.

5 Implementation

Interval construction. Enumerating elements of a consensus set \hat{C}_t in (5) given $\hat{C}_{t,k}$, K , and β is non-trivial if \mathcal{Y} is continuous. We use the following heuristic for regression:

²In [3] the smoothness is parameterized by ρ and we assume $\rho \rightarrow 0$.

instead of enumerating all elements in \mathcal{Y} , we enumerate over the edge of $\hat{C}_{t,k}$ intervals. Let $\hat{C}_{t,k}(\mathbf{x}_t) = [l_{t,k}, u_{t,k}]$. Then, we consider the finite set of candidates $\mathcal{Y}_{\text{candi}} := \{l_{t,k} \mid 1 \leq k \leq K\} \cup \{u_{t,k} \mid 1 \leq k \leq K\}$. Given this, we choose an element voted by at least $K - \beta$ intervals, *i.e.*, $\mathcal{Y}_{\text{maj}} = \{y \in \mathcal{Y}_{\text{candi}} \mid \sum_{k=1}^K \mathbb{1}(y \in \hat{C}_{t,k}(\mathbf{x}_t)) \geq K - \beta\}$. Then, our final interval is $[\min(\mathcal{Y}_{\text{maj}}), \max(\mathcal{Y}_{\text{maj}})]$ if \mathcal{Y}_{maj} is not empty, otherwise $[-\infty, \infty]$. The constructed internal is the over-approximation of $\hat{C}_t(\mathbf{x}_t)$ due to the convexity of intervals (*e.g.*, if the two edge of an interval are voted by $K - \beta$, so all elements between two edges are). For enumerating elements of a base prediction set $\hat{C}_{t,k}(\mathbf{x}_t)$, we use a closed form solution due to the Gaussian distribution, as in [29]. Specifically, given $\tau_{t,k}$ and letting μ and σ be the mean and standard deviation of $s_{t,k}(\mathbf{x}_t, \mathbf{y}_{t,k})$, respectively, we have $\hat{C}_{t,k}(\mathbf{x}_t, \mathbf{y}_{t,k}) = [\mu - \sigma\sqrt{c}, \mu + \sigma\sqrt{c}]$, where $c = -2\ln\tau_{t,k} - 2\ln\sigma - \ln(2\pi)$. If $\hat{C}_{t,k}$ is empty (*i.e.*, $c < 0$), we set $c = 0$.

Ethereum implementation. We implemented ACon² along with MVP and the Kalman filter for each base prediction set in Solidity for the token price application. To this end, we consider multi-thread implementation, while Algorithm 1 assumes a single-thread. In particular, we consider a swap pool based on UniswapV2. Whenever, a swap operation is executed, *i.e.*, `UniswapV2Pair.sol::swap()`, at the k -th pool, we call `update()` in Algorithm 1 at the end of the swap operation, where we use the spot price from the reserves of two tokens as the observation $\mathbf{y}_{t,k}$. During the MVP update, we need a random number generator `rand()`; we use block difficulty and timestamp for the source of randomness, but this can be improved via random number generator oracles. Along with base prediction sets for each pool, we implement a consensus set construction part via (5) in a smart contract, and whenever a user reads the consensus set, K base prediction sets from pre-specified K pools are read. This part is a read-only operation, so it is transaction-free. For fixed point operations, we use the PRBMath math library [5].

We evaluate our Solidity implementation in forked Ethereum mainnet. In particular, we use `anvil` in `foundry` [43] as a local Ethereum node, where it mines a block whenever a transaction arrives. Then, we deploy three AMMs, based on UniswapV2 by initializing reserves of two tokens, along with a customized swap functions as mentioned above. Next, we also deploy the read-only ACon² smart contract. Once the markets by three AMMs are ready, we execute a trader, interfacing with the local blockchain via Web3 libraries, that randomly swaps two tokens from a randomly chosen AMM. Finally, we execute an arbitrageur that exploits the arbitrage opportunity across AMMs, which eventually contributes to balance the prices of three markets. Optionally, we also execute an adversary that chooses an AMM and conducts a huge swap operation to mimic price manipulation.

Hyper-parameters. The proposed adaptive conformal con-

sensus (ACon²) along with base prediction sets (BPS) need to set initial parameters. In particular, a desired miscoverage rate α , the number of sources K , and the number of Byzantine adversaries β are use-specified parameters. Given these parameters, a desired miscoverage for the k -th base prediction set is set by $\frac{\alpha}{K}$. The parameters of MVP are chosen based on suggested in [3]: $\eta = 0.9$, $m = 100$, $r = 1000$, and $\tau_{\max} = 1$. We use the following parameters for the Kalman filter: $\gamma_{\text{noise}} = 10^{-3}$, $w_{0,k}^2 = v_{0,k}^2 = e^{0.1}$. The score $s_{t,k}(\mathbf{x}_t, \mathbf{y}_{t,k})$ is truncated by τ_{\max} if it is larger than τ_{\max} . We use the above parameters for all experiments.

6 Evaluation

We evaluate the efficacy of the proposed ACon² based on two price datasets, which manifest global distribution shift (for Challenge 1, 3 and 4) and local shift due to Byzantine adversaries (for Challenge 1, 2, and 4), and one case study over the Ethereum blockchain (for Challenge 5). Note that we mainly focus on price oracles as it is the current major issue of the oracle problem, but the proposed approach can be applicable in more general setups.

Metric. For evaluation metrics of approaches, we use a miscoverage rate of consensus sets and a size distribution of consensus sets. In particular, the miscoverage rate is $\frac{1}{T} \sum_{t=1}^T \text{Miscover}(\hat{C}_t, \mathbf{x}_t, \mathbf{y}_t)$, as in (4), given a sequence of $(\mathbf{x}_t, \mathbf{y}_t)$ for $1 \leq t \leq T$ at a time horizon T . Here, the consensus label y_t is unknown, so for price data, we choose the median of $\mathbf{y}_{t,k}$ for $1 \leq k \leq K$ as pseudo-consensus labels only for evaluation purposes. The size of a consensus set is measured by a metric $S : 2^{\mathcal{Y}} \rightarrow \mathbb{R}_{\geq 0}$; for the price data, as the consensus set is an interval, we measure the length of the interval.

Baselines. We consider three baselines; a *median baseline* is the median value of values from multiple sources, and a *TWAP_{Keep3rV2} baseline* is the time-weighted average price (TWAP) implemented in Keep3rV2 [9]. These two baselines are not directly comparable to our approach, as it does not quantify uncertainty. But, they are considered to be effective solutions for price manipulation, so we use them in local shift experiments to show their efficacy in price manipulation.

Additionally, we consider a baseline that considers uncertainty. In particular, for the base prediction set, we use one standard deviation prediction set σ -BPS, which returns all labels deviated from the mean by σ , *i.e.*, $\hat{C}_{t,k}(\mathbf{x}_t) := [\mu - \sigma, \mu + \sigma]$, where μ and σ are the mean and standard deviation of a score $s_{t,k}(\mathbf{x}_t, \mathbf{y}_{t,k})$. This base prediction set is used with ACon² for the baseline, denoted by σ -ACon².

6.1 Global Shift: USD/ETH Price Data

We evaluate our approach ACon² in price data that contains global shift. In particular, we use USD/ETH price data from

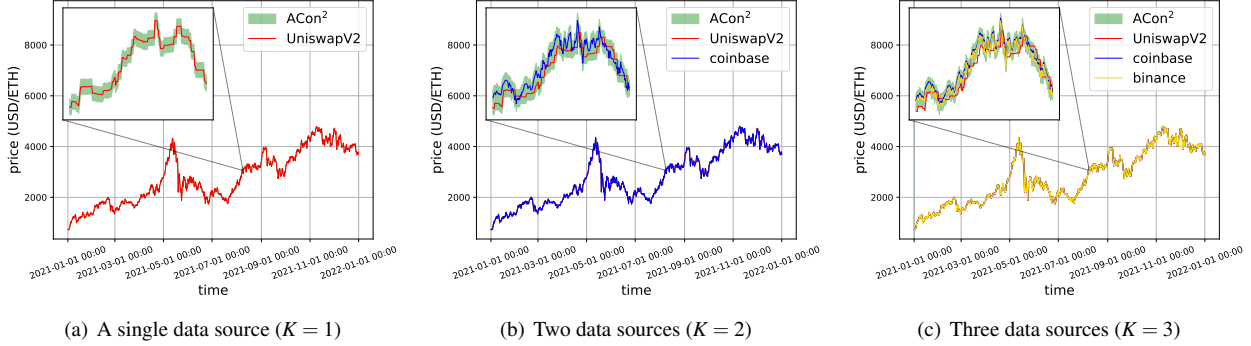


Figure 4: Prediction consensus results on USD/ETH data. The ACon^2 of each figure uses a different number of sources K , as denoted in captions. For any number of sources with $\beta = \lfloor \frac{K}{2} \rfloor$, the ACon^2 finds intervals that closely follow the price of each source, demonstrating that the correctness of the consensus sets by ACon^2 under distribution shift, while maintaining small consensus set size (Challenge ③ and ④). See Figure 5 and 8 for additional details.

2021-1-1 to 2021-12-31 for every 60 seconds, obtained from UniswapV2 via `Web3.py`, Coinbase via Coinbase Pro API, and Binance via Binance API. The results are summarized in Figure 4, Figure 5, and Figure 8.

Figure 4 shows the consensus sets of ACon^2 in green for $K \in \{1, 2, 3\}$, which closely follows the abrupt change of USD/ETH prices, while their interval size is sufficiently small to cover price data from different sources. In particular, the initial part of Figure 4(c) reveals that the consensus sets of ACon^2 when using three sources return ‘I don’t know’ (IDK) intervals, *i.e.*, $[-\infty, \infty]$. this is mainly because a conservative desired miscoverage rate of MVPs on three sources in the early learning stage. In particular, when $K = 3$, we set the desired miscoverage rate of each source by $\frac{\alpha}{3}$, which tends to produce smaller base prediction sets compared to that of $K = 2$. In short, when $K = 3$, the consensus sets provide more precise signals, thus the consensus cannot be achievable.

Figure 5 and 8 demonstrate more details on the correctness guarantee and the efficacy of the consensus sets in their size. In particular, Figure 5 illustrates the miscoverage rate at each time step. Up to the time 200K, the base prediction sets and consensus sets by ACon^2 closely satisfy the desired miscoverage rate. After this time frame, due to the abrupt increase of the USD/ETH price, the miscoverage rates increase, while recovering as time passes. Figure 8 shows the distribution on the size of consensus sets. As can be seen, the set size is mostly 10; considering that the price is not perfectly synchronized due to transaction fee, the set size is reasonable. Here, the consensus sets when $K = 2$ tend to produce larger set size, and this is mainly because of the choice of $\beta = \lfloor \frac{K}{2} \rfloor = 1$, where the consensus set includes all labels from two base prediction sets. In short, from these observation, we empirically justify that ACon^2 closely achieves a desired miscoverage rate, while maintaining a small set size under global shift, addressing Challenge ①, ③ and ④. Finally, see the σ -BPS baseline results in Figure 11 of Appendix D, which shows the

importance of careful parameter adaptation for the correctness guarantee of base prediction sets.

6.2 Local Shift: INV/ETH Price Data

To show the efficacy of our approach under local shift by Byzantine adversaries, we adopt the recent incident on Inverse Fiance [36], which occurs on April 2nd in 2022 and about at \$15.6M was stolen. This incident begins from the price manipulation on the INV-ETH pair of SushiSwap. Interesting, Inverse Finance uses the TWAP oracle by the Keeper [9], but the TWAP oracle was heavily manipulated due to the short time window of the Keeper’s TWAP. We collect the associated price data from Ethereum blockchain between 2022-04-01 and 2022-04-02. In particular, we collect the spot price of Sushiswap and UniswapV2 from all blocks in the time frame. Also, we read the Keeper TWAP oracle data. For the additional source of price, we use Coinbase.

Table 1 illustrates the details on the behavior of our approach, baselines, and price data around the price manipulation. The trend of consensus set results along with the miscoverage rate curve and the size distributions is similar to the USD/ETH data; see Appendix D for the details. Here, we focus on the interpretation of Table 1.

Table 1 includes the price data of INV/ETH from three sources (*i.e.*, SushiSwap, UniswapV2, and Coinbase), baseline results (*i.e.*, the median of three prices and the TWAP of SushiSwap by Keep3rV2), and the consensus sets by ACon^2 with different options on $K \in \{1, 2, 3\}$. Here, the price manipulation occurs around 11:04 on April 2nd, 2022 by swapping 500 ETH for 1.7K INV to the Sushiswap pool, so the spot price of ETH by INV is significantly decreased. Here, the consensus set by ACon^2 ($K = 3$) does not affected by the price manipulation as shown in bold, but in the next time step, it can detect the failure of consensus among three markets, highlighted in blue, producing the IDK interval, $[-\infty, \infty]$;

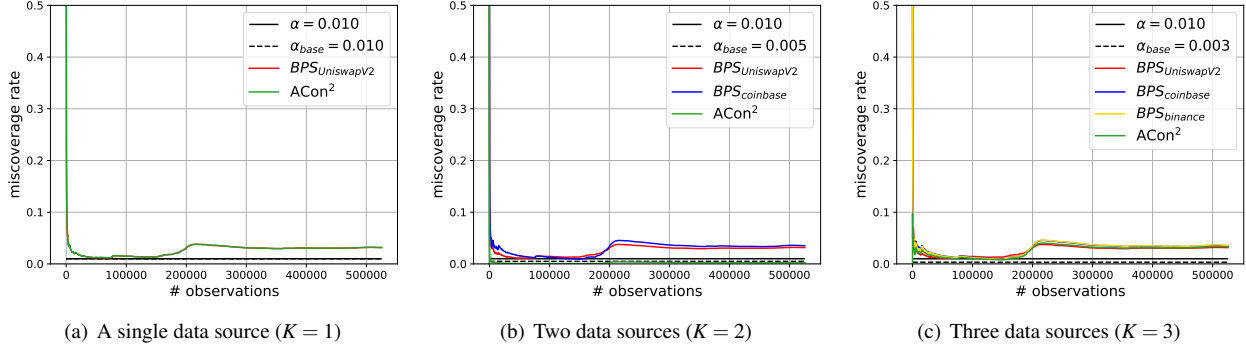


Figure 5: Miscoverage rate on USD/ETH data. For each K , the ACon^2 closely satisfies a desired miscoverage rate α . In particular, for all K , we set a desired miscoverage rate by $\alpha = 0.01$. Moreover, based on Theorem 1, we set the desired miscoverage rate of each base prediction set by $\alpha_{base} = \frac{\alpha}{K}$. As can be seen, the empirical miscoverage rate of each base prediction set is closely converged to α_{base} , thus the empirical miscoverage rate of ACon^2 also tends to converge to α , while affected by the abrupt price change. This demonstrates the approximate correctness of consensus sets by ACon^2 under distribution shift

this demonstrates the positive effect in modeling uncertainty (Challenge ①). The consensus failure is due to the manipulation followed by the slow arbitrageur. Compared to this, the consensus sets by ACon^2 with $K = 2$ is affected by the price manipulation, as shown in the underline, but it still shows the abnormal signal via the larger interval size, also showing the usefulness of uncertainty (Challenge ①). However, when $K = 1$, the consensus set by ACon^2 closely follows the manipulated price, which make sense as the current ACon^2 with $K = 1$ assumes that there is no adversaries (*i.e.*, $\beta = 0$). For the median and TWAP (by Keeper) baselines, they do not provide uncertainty, so it is unclear to capture the unusual event in the markets. Moreover, the TWAP tends to maintain the manipulated price for a while, suggesting that choosing a good time window is crucial. Note that for the INV/ETH pair, we could not identify the Chainlink oracle at the time of the incidence, implying that our approach could be a practical oracle solution for minor tokens.

6.3 Case Study: Ethereum Blockchain

Beyond evaluating our approach on real data, we have demonstrated that our approach can be implementable in blockchains. The application running over blockchains requires to have computational limitations, so using machine learning techniques on blockchains is counter-intuitive at the first place. Here, we implement our approach in Solidity and measure its gas usage on the Ethereum network. In particular, Table 2 shows the average gas usage for 500 transactions. “Swap” means the original swap operation (*i.e.*, UniswapV2 swap), which uses 112,904 gas on average. The base prediction sets (BPS) are attached right at the end of the swap function, which increases the gas usage by about 20 times in the worst case. This is mainly due to the iteration in the MVP algorithm,

which is generally unavoidable in machine learning algorithms. In constructing a consensus set by (5) only requires read operations (*i.e.*, reading from intervals of base prediction sets, written in blockchains after the swap operation), thus it does not require gas for transaction. This case study in the Ethereum blockchain demonstrates that our algorithm based on online machine learning is practically implementable in operation-parsimonious blockchains, addressing Challenge ⑤. Finally, Figure 10 in Appendix D shows the consensus sets on a local Ethereum blockchain with three AMMs, one trader, one arbitrageur, and one adversary. As before, the consensus sets by ACon^2 covers the price data, while robust to price manipulation, shown by spikes in Figure 10(b).

7 Related work

7.1 Blockchain Oracles

The blockchain oracle problem has been considered around the birth of the first smart contract enabled Ethereum blockchain [13]; methods to address this issue also has been proposed [1, 8, 10, 11, 19, 32, 34, 41, 50]. Here, considering that the oracle smart contract is an external data feeder, we view existing methods in two categories: whether data is authenticated, assuming their validity (*data authentication*) and whether data is valid (*data validation*).

Methods providing data authentication mainly propose protocols that deliver un-tampered data (*e.g.*, via TLSNotary proof [34] or via Intel Software Guard Extensions [50]); the blockchains generally do have functionality to proactively establish secure channels toward off-chain, thus external services need to push data into the blockchain in reliable ways.

Along with data authentication approaches, we also need to validate whether data is correct mainly via a voting mechanism or Schelling-point scheme. For the voting mechanism, a (weighted) voting scheme on data $\hat{y}(x) \in \mathcal{Y}$ on possible

³Gas is measured, assuming the worst-case loop in Line 12 of Alg. 2.

time	2022-04-02	2022-04-02	2022-04-02	2022-04-02	2022-04-02	2022-04-02
	11:03:40	11:03:50	11:04:00	11:04:10	11:04:20	11:04:30
SushiSwap	9.3734	9.3734	0.1667	4.5976	4.5976	4.5976
UniswapV2	9.1802	9.1802	9.1802	5.3045	5.3045	5.3045
Coinbase	9.1418	9.1418	9.0041	9.0041	9.0041	9.0041
median	9.1802	9.1802	9.0041	5.3045	5.3045	5.3045
TWAP of SushiSwap by Keep3rV2 [9]	8.8497	8.8497	8.8575	0.1667	0.1667	0.3317
BPS _{SushiSwap}	[9.04,9.71]	[9.04,9.71]	[0.45,1.11]	[4.01,4.67]	[4.25,4.91]	[4.26,4.93]
BPS _{UniswapV2}	[8.94,9.42]	[8.94,9.42]	[8.94,9.42]	[5.32,5.81]	[5.08,5.56]	[5.06,5.55]
BPS _{Coinbase}	[9.05,9.24]	[9.05,9.24]	[8.92,9.11]	[8.91,9.10]	[8.91,9.10]	[8.91,9.10]
ACon ² ($K = 3$)	[9.04,9.42]	[9.04,9.42]	[8.94,9.11]	[−∞,∞]	[−∞,∞]	[−∞,∞]
BPS _{SushiSwap}	[9.28,9.47]	[9.28,9.47]	[0.69,0.87]	[4.25,4.44]	[4.34,4.82]	[4.35,4.84]
BPS _{UniswapV2}	[9.09,9.27]	[9.09,9.27]	[9.09,9.27]	[5.47,5.66]	[5.23,5.42]	[5.21,5.40]
ACon ² ($K = 2$)	[9.09,9.47]	[9.09,9.47]	[0.69,9.27]	[4.25,5.66]	[4.34,5.42]	[4.35,5.40]
BPS _{SushiSwap}	[9.28,9.47]	[9.28,9.47]	[0.69,0.87]	[4.25,4.44]	[4.49,4.67]	[4.50,4.69]
ACon ² ($K = 1$)	[9.28,9.47]	[9.28,9.47]	[0.69,0.87]	[4.25,4.44]	[4.49,4.67]	[4.50,4.69]

Table 1: Prediction consensus results on INV/ETH price manipulation data. The price of SushiSwap in red is manipulated (*i.e.*, 0.1667); the updated consensus set by ACon² is not affected by the manipulation, while the base prediction set for SushiSwap, BPS_{SushiSwap}, follows the manipulated price (*i.e.*, [0.03,0.92]). At the next time step, prices are spread due to arbitrage in blue, resulting in failing to make consensus; thus, ACon² returns the interval for “no consensus” (*i.e.*, [−∞,∞]), which signals abnormality of the market while the median does not provide that; this suggests the importance of quantifying uncertainty (Challenge ①). In short, intervals by ACon² do not meaningfully manipulated by adversaries (Challenge ②), thus providing benefits to downstream applications through quantified uncertainty.

	Swap	Swap+BPS	ACon ² (read)
used gas	112,904.23 ±5,115.41	1,941,755.64 ³ ±160.42	0

Table 2: Average gas used over 500 transactions. A token swap operation (*i.e.*, `swap()` in `UniswapV2Pair.sol`) takes 0.1M gas units, while the swap followed by a base prediction set (BPS) update takes 2M gas units in the worst case due to the loop in Algorithm 2. ACon² consists of read-only operations. This demonstrates that ACon² and BPS are implementable in blockchains (Challenge ⑤).

data choices \mathcal{Y} is mainly used. In particular, Truthcoin [41] and Witnet [10] construct a weighted voting matrix on data choices from which extracts a common vote pattern via singular value decomposition and incentivizes or penalizes inlier or outlier voters, respectively. Augur [32] and Astraea [1] use a reputation token or stakes in general for weighted voting on data choices \mathcal{Y} to achieve consensus. Aeternity [19] reuses blockchain consensus mechanisms (*e.g.*, proof-of-work) for the consensus over data choices. The Schelling-point schemes consider the fact that people tend to choose the same solution without communication, which could be a basis for consensus via robust statistics. In particular, Oracle Security Module by MakerDAO [25] and Chainlink [8] exploit a single or multi-layer median over possible data values (mainly prices), produced by node operators.

Compared to the aforementioned approaches to achieve data validity, we account for uncertainty of real data via online machine learning, providing the correctness guarantee on consensus. Data authentication could be achievable if the pro-

posed algorithm is fully implemented within chain as demonstrated in Section 6.3.

7.2 Consensus Problems

The consensus problem is traditionally considered in a distributed system. In distributed systems, we need a protocol that enables consensus on values (*e.g.*, data files) to maintain state consistency among system nodes even in the existence of faulty nodes; see [17] for a survey. In this paper, we consider each system node as a machine learned predictor. Thus, the goal is to achieve consensus on predicted labels, and we reinterpret and simplify setups in [12, 22, 24, 26, 47] for comparison. The following includes short introduction along with comparison; see Table 3 for the comparison summary.

In Byzantine generals [22], each prediction node (*i.e.*, a lieutenant in the generals metaphor) makes an observation x on the environment (*i.e.*, a lieutenant receives messages from other generals) and predicts a discrete label $\hat{y}(x) \in \mathcal{Y}$ (*e.g.*, whether “attack” or not). Then, label predictions from all prediction nodes are aggregated to predict the true consensus label y (*i.e.*, the original order from a commander). Here, achieving the consensus is non-trivial as a subset of prediction nodes can be Byzantine adversaries. This problem mainly considers applications on computer systems, so a discrete, point prediction is considered; given the true consensus label y , it requires to achieve the exactly same prediction $\hat{y}(x)$ (*i.e.*, $y = \hat{y}(x)$ for all x and y). This correctness guarantee is achievable in deterministic systems, but if x and y are stochastic due to uncertainty or y is continuous, it is not possible. The setup for approximate agreement [12] assumes uncertainty on

problem	predictive consensus	true consensus	correctness on predictive consensus
Byzantine generals [22]	$\hat{y}(x) \in \mathcal{Y}$ (point prediction)	y (discrete)	exactly correct, <i>i.e.</i> , $\forall x, y, y = \hat{y}(x)$
approximate agreement [12]	$\hat{y}(x) \in \mathcal{Y}$ (point prediction)	y (continuous)	approximately correct, <i>i.e.</i> , $\forall x, y, y - \hat{y}(x) \leq \epsilon$
triple modular redundancy [24, 47]	$\hat{y}(x) \in \mathcal{Y}$ (point prediction)	y (discrete)	approximately correct, <i>i.e.</i> , $\mathbb{P}_{x,y}\{y = \hat{y}(x)\} \geq 1 - \epsilon$
abstract sensing [26]	$\hat{C}(x) \subseteq \mathcal{Y}$ (set prediction)	y (continuous)	exactly correct, <i>i.e.</i> , $\forall x, y, y \in \hat{C}(x)$
prediction consensus (ours)	$\hat{C}(x) \subseteq \mathcal{Y}$ (set prediction)	y (discrete or continuous)	$(\alpha, \beta, \epsilon)$ -correct, <i>i.e.</i> , $\mathcal{V}(\mathcal{F}, T, \alpha, \beta, L) \leq \epsilon$

Table 3: Related consensus problems (simplified in a prediction setup for comparison). Each problem relies on different setups and correctness definitions. Prediction consensus explicitly considers a learner L that returns predictive consensus \hat{C} , updated via online machine learning.

x and y along with continuous labels y . In particular, the setup considers that the predicted label is approximately correct, *i.e.*, $|y - \hat{y}(x)| \leq \epsilon$ for all x and y , and some $\epsilon \in \mathbb{R}_{\geq 0}$.

In electronic engineering, a similar consensus concept in designing circuits is considered as triple modular redundancy [24, 47]. This mainly computes the discrete output of redundant circuits from the same input x and the majority of the outputs to produce a single output $\hat{y}(x)$. This setup considers that the predicted consensus label is statistically correct, *i.e.*, $\mathbb{P}_{x,y}\{y = \hat{y}(x)\} \geq 1 - \epsilon$ for some $\epsilon \in [0, 1]$.

In system control, the concept of abstract sensing [26] is used to build fault-tolerant sensor fusion, where we consider the outputs from multiple sensors given the observation x are intervals and denote the intersection over intervals from multiple sensors by a consensus interval $\hat{C}(x)$. This setup assumes the interval should include the consensus label y such that the consensus interval eventually includes the consensus label as well, *i.e.*, $y \in \hat{C}(x)$ for all x and y . But, constructing an interval that must include the consensus label is impractical.

The aforementioned setups consider that distributions over the prediction $\hat{y}(x)$ and the consensus label y are stationary, thus do not explicitly consider an online machine learning setup, where the distributions shift along time.

7.3 Conformal Prediction

Conformal prediction is a method that quantifies the uncertainty of any predictors [49]. The conformal prediction constructs a prediction set that possibly contains the true label with a desired level. Here, we consider variations of conformal prediction under different assumptions on data distributions. See Appendix C.1 for additional related work.

Adaptive conformal prediction. The previous conformal prediction methods consider the non-sequential data, assuming shift among a discrete set of distributions. In sequential data, the data shift is continuous, where the online learning of conformal prediction sets is considered. In particular, adaptive conformal inference updates a desired marginal coverage of

conformal prediction for every time step to have a prediction set that satisfies a coverage on any data from an arbitrarily shifted distribution [18]. Multi-valid prediction construct a prediction set at each time that achieves threshold-calibrated validity as well as the desired marginal coverage [3]. Adaptive conformal prediction methods consider a single data source, where the data distribution can be arbitrarily shifted (also by adversaries). In this paper, we consider the consensus over base conformal prediction sets based on any adaptive conformal prediction methods for multiple data sources.

8 Discussion and Conclusion

This paper proposes an adaptive conformal consensus (ACon²) to address the oracle problem in blockchains to achieve consensus over multiple oracles. In particular, the proposed approach addresses five challenges (❶ handling uncertainty, ❷ consensus under Byzantine adversaries, ❸ consensus under distribution shift, ❹ correctness guarantee on the consensus, and ❺ practicality in blockchains), which are theoretically and empirically justified. The following includes discussion on future directions.

Consensus assumption. Assumption 2 consider a situation where the consensus label distribution is identical to the distribution over source labels. This is likely to be true due to the arbitrageur in price markets, but may not hold in general. One way to relax the assumption is considering a distributionally robust setup, *i.e.*, given $\rho \in \mathbb{R}_{\geq 0}$, assume $D_f(p_t(y_t | \mathbf{x}_t) \| p_t(y_{t,k} | \mathbf{x}_{t,k})) \leq \rho$ for any $t \in \{1, \dots, T\}$ and $k \in \{1, \dots, K\}$, where D_f is f -divergence. This assumption can be used instead of (8) in proving Lemma 3, while finding $p_t(y_t | \mathbf{x}_t)$ is non-trivial.

Efficient base prediction set update. As shown in Table 2, the base prediction set update requires more gas. Considering that the adaptive conformal prediction is a recently developing area [3, 18], we believe that our choice of the base prediction set algorithm is a best possible option, while developing computational efficient algorithms would be interesting.

References

[1] J. Adler, R. Berryhill, A. Veneris, Z. Poulos, N. Veira, and A. Kastania. Astraea: A decentralized blockchain oracle. In *2018 IEEE international conference on internet of things (IThings) and IEEE green computing and communications (GreenCom) and IEEE cyber, physical and social computing (CPSCom) and IEEE smart data (SmartData)*, pages 1145–1152. IEEE, 2018.

[2] A. Angelopoulos, S. Bates, J. Malik, and M. I. Jordan. Uncertainty sets for image classifiers using conformal prediction. *arXiv preprint arXiv:2009.14193*, 2020.

[3] O. Bastani, V. Gupta, C. Jung, G. Noarov, R. Rama-lingam, and A. Roth. Practical adversarial multivalid conformal prediction. In *Advances in Neural Information Processing Systems*, 2022.

[4] S. Bates, A. Angelopoulos, L. Lei, J. Malik, and M. I. Jordan. Distribution-free, risk-controlling prediction sets. *arXiv preprint arXiv:2101.02703*, 2021.

[5] P. R. Berg. Solidity library for advanced fixed-point math. <https://github.com/paulrberg/prb-math>, 2021.

[6] bitcoin.org. Bitcoin. <https://bitcoin.org>, 2009.

[7] V. Buterin. Ethereum: A next-generation smart contract and decentralized application platform. 2014.

[8] Chainlink. Chainlink: Blockchain oracles for hybrid smart contracts. <https://chain.link/>, 2019.

[9] T. K. community. Keep3r v2. <https://etherscan.io/address/0x39b1df026010b5aea781f90542ee19e900f2db15#code>, 2022.

[10] A. S. de Pedro, D. Levi, and L. I. Cuende. Witnet: A decentralized oracle network protocol. *arXiv preprint arXiv:1711.09756*, 2017.

[11] Delphi. Delphi systems. <https://delphi.systems/whitepaper.pdf>.

[12] D. Dolev, N. A. Lynch, S. S. Pinter, E. W. Stark, and W. E. Weihl. Reaching approximate agreement in the presence of faults. *Journal of the ACM (JACM)*, 33(3):499–516, 1986.

[13] ethereum.org. Ethereum. <https://ethereum.org>, 2015.

[14] ethereum.org. Oracles. <https://ethereum.org/en/developers/docs/oracles>, 2022.

[15] H. Finance. Harvest flashloan economic attack post-mortem. <https://medium.com/harvest-finance/harvest-flashloan-economic-attack-post-mortem-3cf900d65217>, 2020.

[16] A. Fisch, T. Schuster, T. Jaakkola, and R. Barzilay. Few-shot conformal prediction with auxiliary tasks, 2021.

[17] M. J. Fischer. The consensus problem in unreliable distributed systems (a brief survey). In *International conference on fundamentals of computation theory*, pages 127–140. Springer, 1983.

[18] I. Gibbs and E. Candès. Adaptive conformal inference under distribution shift, 2021.

[19] Z. Hess, Y. Malahov, and J. Pettersson. Æternity blockchain. <https://aeternity.com/aeternity-blockchainwhitepaper.pdf>, 2017.

[20] Immunefi. Enzyme finance price oracle manipulation bugfix review. <https://medium.com/immunefi/enzyme-finance-price-oracle-manipulation-bug-fix-postmortem-4e1f3d4201b5>, 2021.

[21] R. E. Kalman and R. S. Bucy. New results in linear filtering and prediction theory. 1961.

[22] L. Lamport, R. Shostak, and M. Pease. The byzantine generals problem. *ACM Transactions on Programming Languages and Systems*, 4(3):382–401, 1982.

[23] Z. Lipton, Y.-X. Wang, and A. Smola. Detecting and correcting for label shift with black box predictors. In *International conference on machine learning*, pages 3122–3130. PMLR, 2018.

[24] R. E. Lyons and W. Vanderkulk. The use of triple-modular redundancy to improve computer reliability. *IBM journal of research and development*, 6(2):200–209, 1962.

[25] MakerDAO. Oracle module. <https://docs.makerdao.com/smart-contract-modules/oracle-module>, 2017.

[26] K. Marzullo. Tolerating failures of continuous-valued sensors. *ACM Transactions on Computer Systems (TOCS)*, 8(4):284–304, 1990.

[27] T. of Bits. Accidentally stepping on a defi lego. <https://blog.trailofbits.com/2020/08/05/accidentally-stepping-on-a-defi-lego/>, 2020.

[28] palkeo. The bzx attacks explained. <https://www.palkeo.com/en/projets/ethereum/bzx.html>, 2020.

[29] S. Park, O. Bastani, N. Matni, and I. Lee. Pac confidence sets for deep neural networks via calibrated prediction. In *International Conference on Learning Representations*, 2020. URL <https://openreview.net/forum?id=BJxVI04YvB>.

[30] S. Park, E. Dobriban, I. Lee, and O. Bastani. PAC prediction sets under covariate shift. In *International Conference on Learning Representations*, 2022. URL <https://openreview.net/forum?id=DhP9L8vIyLc>.

[31] S. Park, E. Dobriban, I. Lee, and O. Bastani. Pac prediction sets for meta-learning. *arXiv preprint arXiv:2207.02440*, 2022.

[32] J. Peterson, J. Krug, M. Zoltu, A. K. Williams, and

S. Alexander. Augur: a decentralized oracle and prediction market platform. *arXiv preprint arXiv:1501.01042*, 2015.

[33] A. Podkopaev and A. Ramdas. Distribution-free uncertainty quantification for classification under label shift. *arXiv preprint arXiv:2103.03323*, 2021.

[34] Provable. The provable blockchain oracle for modern dapps. <https://provable.xyz/>, 2015.

[35] S. Rakhlin, O. Shamir, and K. Sridharan. Relax and randomize : From value to algorithms. In F. Pereira, C. Burges, L. Bottou, and K. Weinberger, editors, *Advances in Neural Information Processing Systems*, volume 25. Curran Associates, Inc., 2012. URL <https://proceedings.neurips.cc/paper/2012/file/53adaf494dc89ef7196d73636eb2451b-Paper.pdf>.

[36] rekt. Inverse finance. <https://rekt.news/inverse-finance-rekt/>, 2022.

[37] samczsun. Taking undercollateralized loans for fun and for profit. <https://samczsun.com/taking-undercollateralized-loans-for-fun-and-for-profit>, 2019.

[38] samczsun. Taking undercollateralized loans for fun and for profit. <https://samczsun.com/so-you-want-to-use-a-price-oracle>, 2020.

[39] H. Shimodaira. Improving predictive inference under covariate shift by weighting the log-likelihood function. *Journal of statistical planning and inference*, 90(2):227–244, 2000.

[40] N. Szabo. Smart contracts, 1994.

[41] P. Sztorc. Truthcoin: Peer-to-peer oracle system and prediction marketplace. <https://bitcoinhivemind.com/papers/truthcoin-whitepaper.pdf>, 2015.

[42] Q. Team. \$200 m venus protocol hack analysis. <https://quillhasteam.medium.com/200-m-venus-protocol-hack-analysis-b044af76a1ae>, 2021.

[43] T. F. team. Foundry. <https://github.com/foundry-rs/foundry>, 2021.

[44] R. J. Tibshirani, R. Foygel Barber, E. Candes, and A. Ramdas. Conformal prediction under covariate shift. *Advances in Neural Information Processing Systems*, 32: 2530–2540, 2019.

[45] Uniswap. Uniswap protocol. <https://uniswap.org/>, 2018.

[46] UniswapV2. Oracles. <https://docs.uniswap.org/protocol/V2/concepts/core-concepts/oracles>, 2020.

[47] J. Von Neumann. Probabilistic logics and the synthesis of reliable organisms from unreliable components. *Automata studies*, 34(34):43–98, 1956.

[48] V. Vovk. Conditional validity of inductive conformal predictors. *Machine learning*, 92(2-3):349–376, 2013.

[49] V. Vovk, A. Gammerman, and G. Shafer. *Algorithmic learning in a random world*. Springer Science & Business Media, 2005.

[50] F. Zhang, E. Cecchetti, K. Croman, A. Juels, and E. Shi. Town crier: An authenticated data feed for smart contracts. In *Proceedings of the 2016 ACM SIGSAC conference on computer and communications security*, pages 270–282, 2016.

Appendix

A Lemma and Proofs

A.1 Lemma

The Theorem 1 proof exploits the following lemma. Intuitively, the lemma connects the miscoverage rate of a consensus set to the miscoverage rate of a base prediction set.

Lemma 3. *For any $T \in \mathbb{N}$, $i \in \{0, \dots, T\}$, $k \in \{1, \dots, K\}$, $\mathbf{x}_{1:i}$, $\mathbf{y}_{1:i}$, $y_{1:i}$, $\hat{C}_{1:i,k}$, and $\hat{C}_{1:i}$, if any k -th source learner L_k satisfies*

$$\max_{\substack{p_{i+1} \in \mathcal{P}' \\ e_{i+1} \in \mathcal{E}_\beta}} \mathbb{E} \cdots \max_{\substack{p_T \in \mathcal{P}' \\ e_T \in \mathcal{E}_\beta}} \mathbb{E} \sum_{t=i+1}^T \mathbb{1}(\mathbf{Y}_{t,k} \notin \hat{C}_{t,k}(e_t(\mathbf{X}_t))) \leq \delta_{i,k}, \quad (7)$$

where the t -th expectation for $i+1 \leq t \leq T$ is taken over $\mathbf{X}_t \sim p_t(\mathbf{x})$, $\mathbf{Y}_t \sim p_t(\mathbf{y} | e_t(\mathbf{X}_t))$, and $\hat{C}_{t,k} \sim L_k(\mathbf{x}_{1:t-1}, \mathbf{y}_{1:t-1, k}, \hat{C}_{1:t-1, k})$, then a consensus learner L satisfies

$$\max_{\substack{p_{i+1} \in \mathcal{P} \\ e_{i+1} \in \mathcal{E}_\beta}} \mathbb{E} \cdots \max_{\substack{p_T \in \mathcal{P} \\ e_T \in \mathcal{E}_\beta}} \mathbb{E} \sum_{t=i+1}^T \mathbb{1}(Y_t \notin \hat{C}_t(e_t(\mathbf{X}_t))) \leq \max_{\mathcal{S}_{i+1:T} \in \mathcal{K}_{K-\beta}^{T-i}} \sum_{k \in \mathcal{S}_i} \delta_{i,k} \leq \sum_{k=1}^K \delta_{i,k},$$

where $\mathcal{K}_{K-\beta} := \{\mathcal{S} \subseteq \{1, \dots, K\} \mid |\mathcal{S}| \geq K - \beta\}$ and the t -th expectation for $i+1 \leq t \leq T$ is taken over $\mathbf{X}_t \sim p_t(\mathbf{x})$, $\mathbf{Y}_t \sim p_t(\mathbf{y} | e_t(\mathbf{X}_t))$, $Y_t \sim p_t(y | \mathbf{X}_t)$, and $\hat{C}_t \sim L(\mathbf{x}_{1:t-1}, \mathbf{y}_{1:t-1}, \hat{C}_{1:t-1})$.

A.2 Proof of Lemma 3

For any $t \in \{i+1, \dots, T\}$, $\bar{p}_t \in \mathcal{P}$, $\bar{p}'_t \in \mathcal{P}'$, and $\bar{e}_t \in \mathcal{E}_\beta$, we have

$$\max_{\substack{p_{i+1} \in \mathcal{P} \\ e_{i+1} \in \mathcal{E}_\beta}} \mathbb{E} \cdots \max_{\substack{p_T \in \mathcal{P} \\ e_T \in \mathcal{E}_\beta}} \mathbb{E} \sum_{t=i+1}^T \mathbb{1}(Y_t \in \hat{C}_t(e_t(\mathbf{X}_t))) \geq \sum_{t=i+1}^T \mathbb{P}\{Y_t \in \hat{C}_t(\bar{e}_t(\mathbf{X}_t))\},$$

where the probability at time t is take over $\mathbf{X}_t \sim \bar{p}_t(\mathbf{x})$, $\mathbf{Y}_t \sim \bar{p}_t(\mathbf{y} | \bar{e}_t(\mathbf{X}_t))$, $Y_t \sim \bar{p}_t(y | \mathbf{X}_t)$, and $\hat{C}_t \sim L(\mathbf{x}_{1:t-1}, \mathbf{y}_{1:t-1}, \hat{C}_{1:t-1})$, and we also have

$$\delta_{i,k} \geq \max_{\substack{p_{i+1} \in \mathcal{P}' \\ e_{i+1} \in \mathcal{E}_\beta}} \mathbb{E} \cdots \max_{\substack{p_T \in \mathcal{P}' \\ e_T \in \mathcal{E}_\beta}} \mathbb{E} \sum_{t=i+1}^T \mathbb{1}(\mathbf{Y}_{t,k} \notin \hat{C}_{t,k}(e_t(\mathbf{X}_t))) \geq \sum_{t=i+1}^T \mathbb{P}\{\mathbf{Y}_{t,k} \notin \hat{C}_t(\bar{e}_t(\mathbf{X}_t))\},$$

where the probability at time t is take over $\mathbf{X}_t \sim \bar{p}'_t(\mathbf{x})$, $\mathbf{Y}_t \sim \bar{p}'_t(\mathbf{y} | \bar{e}_t(\mathbf{X}_t))$, and $\hat{C}_{t,k} \sim L_k(\mathbf{x}_{1:t-1}, \mathbf{y}_{1:t-1, k}, \hat{C}_{1:t-1, k})$,

Then, letting $\mathcal{S}_t^* \in \mathcal{K}_{K-\beta}$ be a set of indices of sources which are not manipulated by a β -Byzantine adversary at time t , we

have

$$\begin{aligned}
\sum_{t=i+1}^T \mathbb{P} \{ Y_t \in \hat{C}_t(\bar{e}_t(\mathbf{X}_t)) \} &= \sum_{t=i+1}^T \mathbb{P} \left\{ \sum_{k=1}^K \mathbb{1} (Y_t \in \hat{C}_{t,k}(\bar{e}_t(\mathbf{X}_t))) \geq K - \beta \right\} \\
&= \sum_{t=i+1}^T \mathbb{P} \left\{ \bigvee_{S \in \mathcal{K}_{K-\beta}} \bigwedge_{k \in S} (Y_t \in \hat{C}_{t,k}(\bar{e}_t(\mathbf{X}_t))) \right\} \\
&\geq \sum_{t=i+1}^T \mathbb{P} \left\{ \bigwedge_{k \in \mathcal{S}_t^*} (Y_t \in \hat{C}_{t,k}(\bar{e}_t(\mathbf{X}_t))) \right\} \\
&= T - \sum_{t=i+1}^T \mathbb{P} \left\{ \bigvee_{k \in \mathcal{S}_t^*} (Y_t \notin \hat{C}_{t,k}(\bar{e}_t(\mathbf{X}_t))) \right\} \\
&\geq T - \sum_{t=i+1}^T \sum_{k \in \mathcal{S}_t^*} \mathbb{P} \{ Y_t \notin \hat{C}_{t,k}(\bar{e}_t(\mathbf{X}_t)) \} \\
&= T - \sum_{t=i+1}^T \sum_{k \in \mathcal{S}_t^*} \mathbb{P} \{ \mathbf{Y}_{t,k} \notin \hat{C}_{t,k}(\bar{e}_t(\mathbf{X}_t)) \} \\
&\geq T - \sum_{t=i+1}^T \max_{S_t \in \mathcal{K}_{K-\beta}} \sum_{k \in S_t} \mathbb{P} \{ \mathbf{Y}_{t,k} \notin \hat{C}_{t,k}(\bar{e}_t(\mathbf{X}_t)) \} \\
&= T - \max_{S_{i+1:T} \in \mathcal{K}_{K-\beta}^{T-i}} \sum_{t=i+1}^T \sum_{k \in S_t} \mathbb{P} \{ \mathbf{Y}_{t,k} \notin \hat{C}_{t,k}(\bar{e}_t(\mathbf{X}_t)) \} \\
&= T - \max_{S_{i+1:T} \in \mathcal{K}_{K-\beta}^{T-i}} \sum_{k \in S_j} \sum_{t=i+1}^T \mathbb{P} \{ \mathbf{Y}_{t,k} \notin \hat{C}_{t,k}(\bar{e}_t(\mathbf{X}_t)) \} \\
&\geq T - \max_{S_{i+1:T} \in \mathcal{K}_{K-\beta}^{T-i}} \sum_{k \in S_j} \delta_{i,k},
\end{aligned} \tag{8}$$

as claimed.

A.3 Proof of Theorem 1

To avoid clutter, consider that the expectation at time t is take over $\mathbf{X}_t \sim p_t(\mathbf{x})$, $\mathbf{Y}_t \sim p_t(\mathbf{y} \mid e_t(\mathbf{X}_t))$, $Y_t \sim p_t(y \mid \mathbf{X}_t)$, and $\hat{C}_t \sim L(\mathbf{z}_{1:t-1})$. We first prove a general statement; for any $i \in \{1, \dots, T\}$, we have

$$\begin{aligned}
T\epsilon_{T,k} &\geq T\mathcal{V}_k(\mathcal{F}_k, T, \alpha_k, \beta, L_k) \\
&\geq \sum_{t=1}^i \mathbb{1} (\mathbf{y}_{t,k} \notin \hat{C}_{t,k}(e_t(\mathbf{x}_t))) + \max_{\substack{p_{i+1} \in \mathcal{P}' \\ e_{i+1} \in \mathcal{E}_\beta}} \mathbb{E} \cdots \max_{\substack{p_T \in \mathcal{P}' \\ e_T \in \mathcal{E}_\beta}} \mathbb{E} \sum_{t=i+1}^T \mathbb{1} (\mathbf{Y}_{t,k} \notin \hat{C}_{t,k}(e_t(\mathbf{X}_t))) - T\alpha_k
\end{aligned}$$

for some $(e_t(\mathbf{x}_1), \dots, e_t(\mathbf{x}_i))$, $(\mathbf{y}_{1,k}, \dots, \mathbf{y}_{i,k})$, and $(\hat{C}_{1,k}, \dots, \hat{C}_{i,k})$. Thus, we have

$$\max_{\substack{p_{i+1} \in \mathcal{P}' \\ e_{i+1} \in \mathcal{E}_\beta}} \mathbb{E} \cdots \max_{\substack{p_T \in \mathcal{P}' \\ e_T \in \mathcal{E}_\beta}} \mathbb{E} \sum_{t=i+1}^T \mathbb{1} (\mathbf{Y}_{t,k} \notin \hat{C}_{t,k}(e_t(\mathbf{X}_t))) \leq T\epsilon_{T,k} + T\alpha_k - \sum_{t=1}^i \mathbb{1} (\mathbf{y}_{t,k} \notin \hat{C}_{t,k}(e_t(\mathbf{x}_t))).$$

Due to Lemma 3,

$$\begin{aligned}
\max_{\substack{p_{i+1} \in \mathcal{P} \\ e_{i+1} \in \mathcal{E}_\beta}} \mathbb{E} \cdots \max_{\substack{p_T \in \mathcal{P} \\ e_T \in \mathcal{E}_\beta}} \mathbb{E} \sum_{t=i+1}^T \mathbb{1} (Y_t \notin \hat{C}_t(e_t(\mathbf{X}_t))) &\leq \sum_{k=1}^K \left(T\epsilon_{T,k} + T\alpha_k - \sum_{t=1}^i \mathbb{1} (\mathbf{y}_{t,k} \notin \hat{C}_{t,k}(e_t(\mathbf{x}_t))) \right) \\
&= \sum_{k=1}^K T\epsilon_{T,k} + \sum_{k=1}^K T\alpha_k - \sum_{k=1}^K \sum_{t=1}^i \mathbb{1} (\mathbf{y}_{t,k} \notin \hat{C}_{t,k}(e_t(\mathbf{x}_t)))
\end{aligned}$$

By rearranging terms, we have

$$\sum_{k=1}^K \sum_{t=1}^i \mathbb{1}(\mathbf{y}_{t,k} \notin \hat{C}_{t,k}(e_t(\mathbf{x}_t))) + \max_{\substack{p_{i+1} \in \mathcal{P} \\ e_{i+1} \in \mathcal{E}_\beta}} \mathbb{E} \cdots \max_{\substack{p_T \in \mathcal{P} \\ e_T \in \mathcal{E}_\beta}} \mathbb{E} \sum_{t=i+1}^T \mathbb{1}(Y_t \notin \hat{C}_t(e_t(\mathbf{X}_t))) - \sum_{k=1}^K T \alpha_k \leq \sum_{k=1}^K T \varepsilon_{T,k}.$$

By setting $i = 0$, we have

$$\frac{1}{T} \max_{\substack{p_1 \in \mathcal{P} \\ e_1 \in \mathcal{E}_\beta}} \mathbb{E} \cdots \max_{\substack{p_T \in \mathcal{P} \\ e_T \in \mathcal{E}_\beta}} \mathbb{E} \sum_{t=1}^T \mathbb{1}(Y_t \notin \hat{C}_t(e_t(\mathbf{X}_t))) - \sum_{k=1}^K \alpha_k \leq \sum_{k=1}^K \varepsilon_{T,k},$$

as claimed.

A.4 Proof of Lemma 1

We have

$$\mathcal{V}_k(\mathcal{F}_k, T, \alpha_k, \beta, L_k) = \max_{\substack{p_1 \in \mathcal{P} \\ e_1 \in \mathcal{E}_\beta \\ \hat{C}_{1,k} \sim L_k(\cdot)}} \mathbb{E}_{\substack{\mathbf{X}_1 \sim p_1(\mathbf{x}) \\ \mathbf{Y}_{1,k} \sim p_1(\mathbf{y}_k | e_1(\mathbf{X}_1))}} \cdots \max_{\substack{p_T \in \mathcal{P} \\ e_T \in \mathcal{E}_\beta \\ \hat{C}_{T,k} \sim L_k(\cdot)}} \mathbb{E}_{\substack{\mathbf{X}_T \sim p_T(\mathbf{x}) \\ \mathbf{Y}_{T,k} \sim p_T(\mathbf{y}_k | e_T(\mathbf{X}_T))}} \left\{ \frac{1}{T} \sum_{t=1}^T \mathbb{1}(\mathbf{Y}_{t,k} \notin \hat{C}_{t,k}(e_t(\mathbf{X}_t))) - \alpha \right\} \quad (9)$$

$$\begin{aligned} &\leq \max_{\substack{p_1 \in \mathcal{P}' \\ \hat{C}_{1,k} \sim L_k(\cdot)}} \mathbb{E}_{(\mathbf{X}_1, \mathbf{Y}_{1,k}) \sim p_1} \cdots \max_{\substack{p_T \in \mathcal{P}' \\ \hat{C}_{T,k} \sim L_k(\cdot)}} \mathbb{E}_{(\mathbf{X}_T, \mathbf{Y}_{T,k}) \sim p_T} \left\{ \frac{1}{T} \sum_{t=1}^T \mathbb{1}(\mathbf{Y}_{t,k} \notin \hat{C}_{t,k}(\mathbf{X}_t)) - \alpha \right\} \\ &\leq \max_{\substack{p_1 \in \mathcal{P}' \\ \hat{C}_{1,k} \sim L_k(\cdot)}} \mathbb{E}_{(\mathbf{X}_1, \mathbf{Y}_{1,k}) \sim p_1} \cdots \max_{\substack{p_T \in \mathcal{P}' \\ \hat{C}_{T,k} \sim L_k(\cdot)}} \mathbb{E}_{(\mathbf{X}_T, \mathbf{Y}_{T,k}) \sim p_T} \left| \frac{1}{T} \sum_{t=1}^T \mathbb{1}(\mathbf{Y}_{t,k} \notin \hat{C}_{t,k}(\mathbf{X}_t)) - \alpha \right| \\ &= \mathcal{V}'(\mathcal{F}_k, T, \alpha_k, L_k). \end{aligned} \quad (10)$$

Here, the first inequality holds as the Byzantine adversaries e_i for $i \in \{1, \dots, T\}$ may not choose to manipulate examples for the k -th source in (9), but (10) is equivalent to always manipulating examples for the k -th source due to the maximum over \mathcal{P}' , thus forming an upper bound.

A.5 Proof of Lemma 2

Let $m = |\mathcal{F}|$, $B_i = [\frac{i-1}{m}, \frac{i}{m})$, $B_m = [\frac{m-1}{m}, 1]$, $S_i = \{t \in \{1, \dots, T\} \mid \tau_t \in B_i\}$, $f(n) := \sqrt{(n+1) \log_2^2(n+2)}$, and $K_1 = \sum_{n=0}^{\infty} \frac{1}{f(n)^2}$. Based on Theorem 3.1 of [3], the MVP learner is threshold calibrated multivalid, which means that for all $i \in \{1, \dots, m\}$ the value of the learner is bounded as follows:

$$\max_{\substack{p_1 \in \mathcal{P}' \\ \hat{C}_1 \sim L_{\text{MVP}}(\cdot)}} \mathbb{E}_{(X_1, Y_1) \sim p_1} \cdots \max_{\substack{p_T \in \mathcal{P}' \\ \hat{C}_T \sim L_{\text{MVP}}(\cdot)}} \mathbb{E}_{(X_T, Y_T) \sim p_T} \left| \frac{1}{|S_i|} \sum_{t \in S_i} \text{Miscover}(\hat{C}_t, X_t, Y_t) - \alpha \right| \leq \frac{f(|S_i|)}{|S_i|} \sqrt{4K_1 m \ln m}$$

if the distribution over scores $s_t(X_t, Y_t)$ for any $t \in \{1, \dots, T\}$ is smooth enough and $\eta = \sqrt{\frac{\ln m}{2K_1 m}}$. Thus, we have

$$\begin{aligned}
\mathcal{V}'(\mathcal{F}, T, \alpha, L_{\text{MVP}}) &= \max_{\substack{p_1 \in \mathcal{P}' \\ \hat{C}_1 \sim L_{\text{MVP}}(\cdot)}} \dots \max_{\substack{p_T \in \mathcal{P}' \\ \hat{C}_T \sim L_{\text{MVP}}(\cdot)}} \left| \frac{1}{T} \sum_{t=1}^T \text{Miscover}(\hat{C}_t, X_t, Y_t) - \alpha \right| \\
&= \max_{\substack{p_1 \in \mathcal{P}' \\ \hat{C}_1 \sim L_{\text{MVP}}(\cdot)}} \dots \max_{\substack{p_T \in \mathcal{P}' \\ \hat{C}_T \sim L_{\text{MVP}}(\cdot)}} \left| \frac{1}{T} \sum_{t=1}^T (\text{Miscover}(\hat{C}_t, X_t, Y_t) - \alpha) \right| \\
&= \max_{\substack{p_1 \in \mathcal{P}' \\ \hat{C}_1 \sim L_{\text{MVP}}(\cdot)}} \dots \max_{\substack{p_T \in \mathcal{P}' \\ \hat{C}_T \sim L_{\text{MVP}}(\cdot)}} \left| \frac{1}{T} \sum_{i=1}^m S_i \frac{1}{S_i} \sum_{t \in S_i} (\text{Miscover}(\hat{C}_t, X_t, Y_t) - \alpha) \right| \\
&\leq \max_{\substack{p_1 \in \mathcal{P}' \\ \hat{C}_1 \sim L_{\text{MVP}}(\cdot)}} \dots \max_{\substack{p_T \in \mathcal{P}' \\ \hat{C}_T \sim L_{\text{MVP}}(\cdot)}} \frac{1}{T} \sum_{i=1}^m S_i \left| \frac{1}{S_i} \sum_{t \in S_i} (\text{Miscover}(\hat{C}_t, X_t, Y_t) - \alpha) \right| \\
&\leq \max_{\substack{p_1 \in \mathcal{P}' \\ \hat{C}_1 \sim L_{\text{MVP}}(\cdot)}} \dots \max_{\substack{p_T \in \mathcal{P}' \\ \hat{C}_T \sim L_{\text{MVP}}(\cdot)}} \frac{1}{T} \sum_{i=1}^m T \left| \frac{1}{S_i} \sum_{t \in S_i} (\text{Miscover}(\hat{C}_t, X_t, Y_t) - \alpha) \right| \\
&\leq \sum_{i=1}^m \max_{\substack{p_1 \in \mathcal{P}' \\ \hat{C}_1 \sim L_{\text{MVP}}(\cdot)}} \dots \max_{\substack{p_T \in \mathcal{P}' \\ \hat{C}_T \sim L_{\text{MVP}}(\cdot)}} \left| \frac{1}{S_i} \sum_{t \in S_i} (\text{Miscover}(\hat{C}_t, X_t, Y_t) - \alpha) \right| \\
&\leq \sum_{i=1}^m \frac{f(|S_i|)}{|S_i|} \sqrt{4K_1 m \ln m},
\end{aligned}$$

as claimed, considering that $3.3 \leq K_1 \leq 3.4$.

B MVP Algorithm

C Additional Related Work

C.1 Conformal Prediction

No shift. The original conformal prediction assumes exchangeability on data (where the special case is the independent and identical distribution (i.i.d.) assumption on data). This mainly assumes that in prediction, the conformal predictor observes the data which are drawn from the same distribution as in training. Under this assumption, a marginal coverage guarantee [2, 49] and a conditional coverage guarantee (*i.e.*, probably approximately correct (PAC) guarantee) [4, 29, 48] can be achievable for the correctness of constructed prediction sets. However, this strong assumption on the no distribution shift can be broken in practice.

Covariate or label shift. To address the no shift assumption, the conformal prediction approach can be extended to handle covariate shift [39], where the covariate distribution $p(x)$ can be shifted in prediction, while the labeling distribution $p(y|x)$ is unchanged, or label shift [23], where the label distribution $p(y)$ can be shifted in prediction, while the conditional covariate distribution $p(x|y)$ is not changing. In particular, weighted conformal prediction can achieve a desired marginal coverage rate given importance weights [44]; similarly, PAC prediction sets, also called training-conditional inductive conformal prediction, achieves a desired PAC guarantee under a smoothness assumption on distributions [30]. The conformal prediction can achieve the marginal coverage guarantee under label shift by exploiting importance weights [33].

Meta learning. Covariate and label shift setups involve two distributions, while multiple distributions for each data sources can be considered in a meta learning setup. In meta learning, multiple data sources are considered, assuming a distribution of each data source are drawn from the same distribution. Under this setup, a conformal prediction tailored to meta learning can attain a desired coverage guarantee [16], a conditional guarantee [16], a fully-conditional guarantee [31].

Algorithm 2 MVP [3] for the k -th source

```

1: procedure UPDATEMVP( $\hat{C}_{t,k}$ ,  $\mathbf{x}_t$ ,  $\mathbf{y}_{t,k}$ ;  $\eta$ )
2:    $n \leftarrow n_{t,k}$ 
3:    $v \leftarrow v_{t,k}$ 
4:    $err \leftarrow \mathbb{1} (\mathbf{y}_{t,k} \notin \hat{C}_{t,k}(\mathbf{x}_t))$ 
5:    $n_i \leftarrow n_i + 1$  if  $\tau_{t,k}$  is in the  $i$ -th bin
6:    $v_i \leftarrow v_i + \alpha - err$  if  $\tau_{t,k}$  is in the  $i$ -th bin
7:    $w_0 \leftarrow e^{\eta v_0 / f(n_0)} - e^{-\eta v_0 / f(n_0)}$ 
8:   if  $w_0 > 0$  then
9:      $pos \leftarrow True$ 
10:   else
11:      $pos \leftarrow False$ 
12:   for  $i = 1, \dots, m-1$  do
13:      $w_i \leftarrow e^{\eta v_i / f(n_i)} - e^{-\eta v_i / f(n_i)}$ 
14:     if  $w_i > 0$  then
15:        $pos \leftarrow True$ 
16:     if  $w_i \cdot w_{i-1} \leq 0$  then
17:       if  $|w_i| + |w_{i-1}| = 0$  then
18:          $b_i \leftarrow 1$ 
19:       else
20:          $b_i \leftarrow \frac{|w_i|}{|w_i| + |w_{i-1}|}$ 
21:       if  $rand() \leq b_i$  then
22:          $\tau_{t+1,k} \leftarrow \tau_{\max} \left( \frac{i}{m} - \frac{1}{rm} \right)$ 
23:         return  $1 - \tau_{t+1,k}$ 
24:       else
25:          $\tau_{t+1,k} \leftarrow \tau_{\max} \frac{i}{m}$ 
26:         return  $1 - \tau_{t+1,k}$ 
27:   if  $pos$  then
28:      $\tau_{t+1,k} \leftarrow \tau_{\max}$ 
29:   else
30:      $\tau_{t+1,k} \leftarrow 0$ 
31:   return

```

D Additional Results

We added additional results on the INV/ETH data. See the captions for details on each figures.

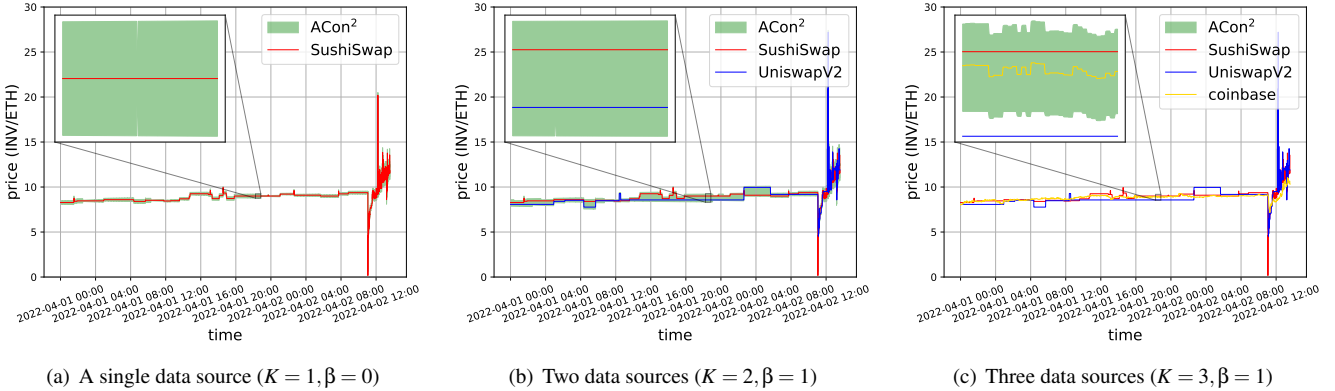


Figure 6: Prediction consensus results on INV/ETH price manipulation data. For $K \in \{1, 2, 3\}$, the consensus sets by ACon^2 closely follow the price data, but when price manipulation occurs, the behaviors of consensus sets differ. In particular, when $K = 3$, the consensus sets are not meaningfully manipulated by the Byzantine adversaries, while the consensus sets for $K = 1$ and $K = 2$ are affected by the adversaries. See Table 1 for the detailed analysis on the consensus sets under manipulation.

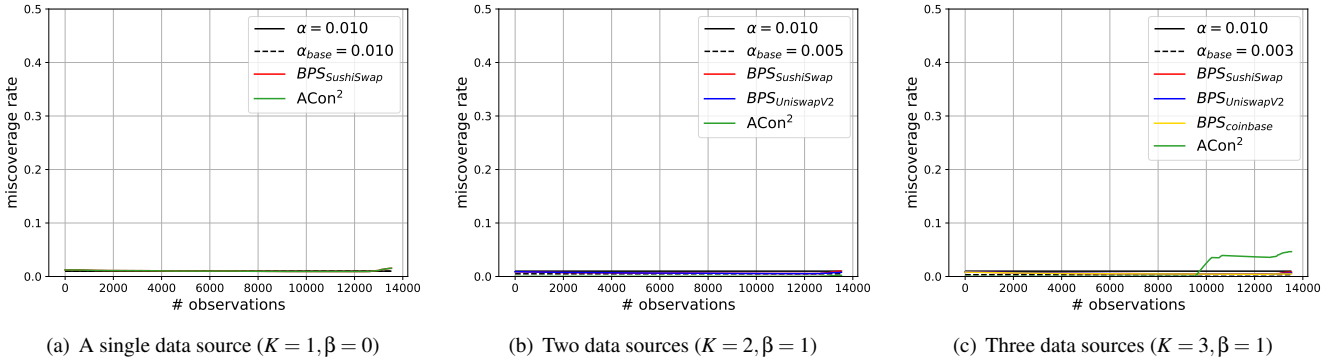


Figure 7: Miscoverage rate on INV/ETH data. The miscoverage rate of base prediction sets and consensus sets closely follow the desired coverage rate, where α_{base} and α are the desired miscoverage rate of the base prediction sets and consensus sets, respectively. In Figure 7(c), the miscoverage rate of the consensus sets is dramatically increased, which is mainly because of the pseudo-consensus labels and tight consensus sets; in particular, the true consensus label is unknown, so we use the pseudo-consensus label. But, around time step 10K the consensus set is tight, while the pseudo-consensus label is not included; this may not necessarily imply that the consensus set is incorrect.

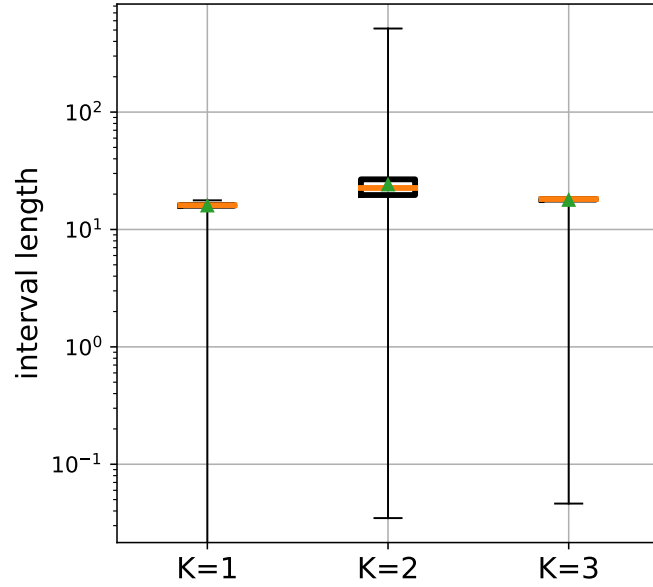


Figure 8: Size distributions of consensus sets on USD/ETH data. Here, we do not count the IDK intervals, where the 0.062% of consensus sets when $K = 3$ are the IDK intervals. As can be seen, the consensus set is relatively small when $K = 1$ and $K = 3$, but the consensus sets by $K = 1$ are prone to manipulation.

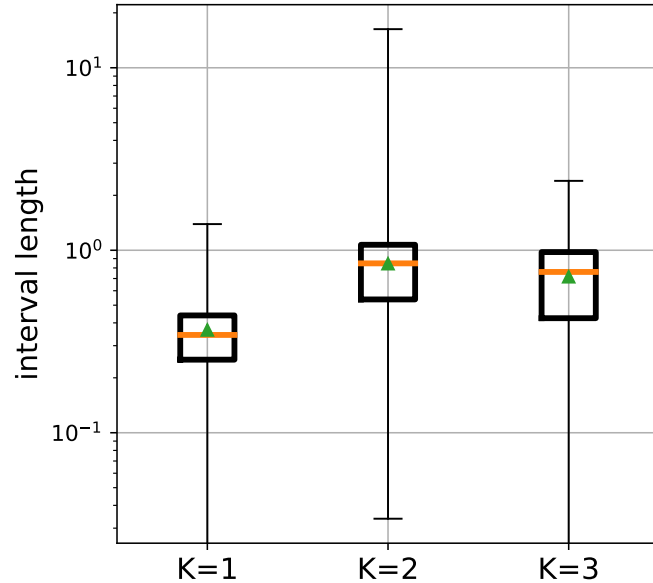


Figure 9: Size distributions of consensus sets on INV/EHT data. Here, we do not count for the IDK intervals, where the 0.6% of the consensus sets when $K = 3$ are the IDK intervals. The consensus sets are mostly less than one, which looks reasonable, considering the price scale. The consensus sets when $K = 1$ tends to be smaller than others, but the sets are prone to adversarial manipulation.

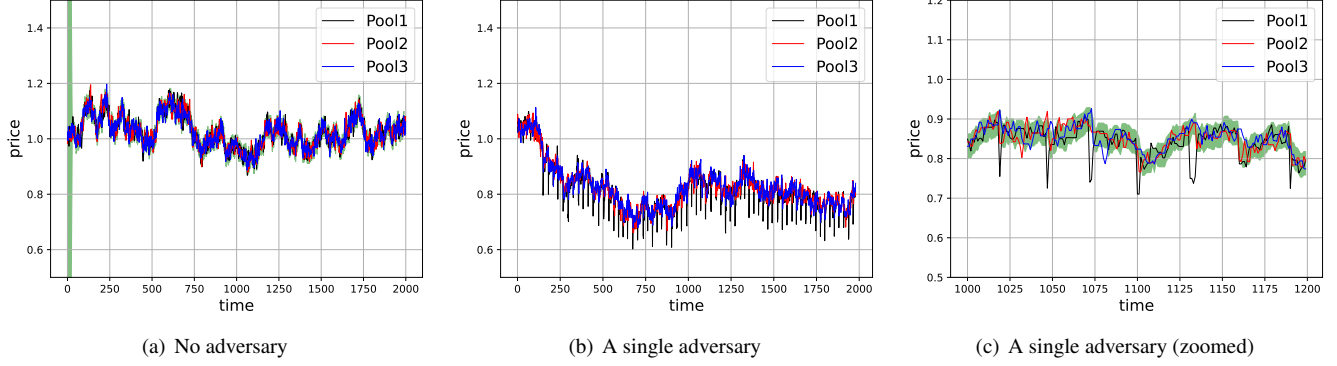


Figure 10: Prediction consensus results on Ethereum network data. As mentioned in Section 5, we establish a simulated environment on the Ethereum network for evaluating our approach. This environment consists of three AMMs, one trader, one arbitrageur, and optionally one adversary. Figure 10(a) shows the price of two tokens without an adversary. As can be seen, the prices from three AMMs are synchronized due to the arbitrageur. Figure 10(b) shows the price trend in manipulation attempts. Along with Figure 10(c), the consensus sets by ACon^2 with $K = 3$ achieves the consensus among price data even in the presence of the adversary.

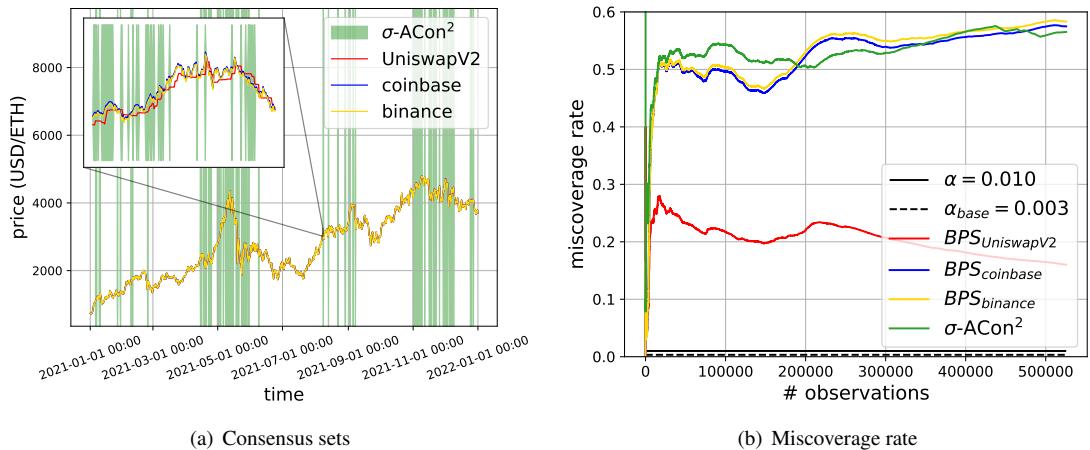


Figure 11: σ -BPS results on USD/ETH data. We apply σ -BPS along with ACon^2 , denoted by $\sigma\text{-ACon}^2$. Figure 11(a) demonstrates that the baseline produces many IDK intervals, meaning that it does not conclude consensus (which is possible as demonstrated by our approach). This is mainly because the σ -BPS does not produce correct intervals. Figure 11(b) shows the miscoverage rate, which is around 0.5. This means that the intervals by the baseline miscovers the half of data, illustrating that the baseline does not provide control over the correctness guarantee.